University of Cyprus
Department of Biological Sciences

"*InvasiCell* is a physiologically relevant *in vitro* model for the study of tumor progression and the evaluation of potential cancer medications more accurately than current in *vitro assays*."

Alexandra Manoli

A Research-Based Master's Thesis
for the
Degree of Magister Scientiae in Biomedical Sciences

May 30, 2024

ABSTRACT

Cancer cases have been constantly increasing over the past few decades, leading it to become the second cause of lethality worldwide, with cancer metastasis being responsible for approximately 90% of cancer-related deaths. Thus, cancer research is essential to enhance our knowledge of the underlying mechanisms that drive tumor progression and metastasis in order to enable the development of new anti-cancer therapies. However, even though *in vivo* and *in vitro* models that are currently used in cancer research have provided valuable information on cancer progression, only a few therapies that show promise *in vitro* studies eventually prove efficacious in clinical studies. Consequently, several studies emphasize the limitations of *in vitro* models, which are currently used in cancer research, and highlight the need for the development of new more physiologically relevant *in vitro* models for the study of tumor progression and evaluating the efficacy of potential new anti-cancer medications. The aim of this study was to examine whether *InvasiCell*, a novel device and associated *in vitro* assay that were developed in our lab, can be used as a physiologically relevant model to study various aspects of tumor progression, compared to the existing *in vitro* tools that are currently used in cancer research. Specifically, wound healing assays, Boyden chamber assays, *InvasiCell*, and tumor spheroids, were used to evaluate the *in vitro* invasive potential of previously characterized breast and pancreatic cancer cell lines with known *in vivo* metastatic potential. The collective data from this study suggest that *InvasiCell* reflects the *in vivo* metastatic potential of the evaluated cell lines more accurately and reliably than other assays. Additionally, given that fibroblasts are the most abundant stromal cell type in the tumor microenvironment and their role in tumor progression is controversial, we used *InvasiCell* to examine whether the presence of NIH3T3 fibroblasts could affect tumor cell invasive capacity and potentially improve our ability to predict the metastatic potential of tumor cells. Our findings indicate that the inclusion of fibroblasts with cancer cells reduces the invasion potential of various breast cancer cell lines tested. Finally, to examine if *InvasiCell* could be used as a drug response assay, we treated breast cancer cell lines with previously established concentrations of Doxorubicin Hydrochloride under normal tissue conditions or within *InvasiCell*. We observed that the cells within *InvasiCell* displayed enhanced drug resistance, which resembles previously published studies performed with spheroid assays. Collectively,

InvasiCell can effectively distinguish cell lines with different metastatic capacities, allow researchers to examine tumor cell behavior and interactions by performing co-culture experiments with other cell types, and study cellular resistance to various drugs. Therefore, *InvasiCell* is a promising tool for cancer research, which could enhance our knowledge and understanding of critical steps in tumor progression and facilitate the development of more effective anti-cancer strategies and therapies.

ACKNOWLEDGEMENTS

Firstly, I would like to thank my research supervisor Professor Paris A. Skourides for providing me the opportunity to undertake my MSc studies at his research laboratory and for trusting me for the development of this project. His constant guidance, encouragement, and support were helpful and important throughout my studies as a member of his lab. Additionally, I would like to thank Dr. Crysoula Pitsouli and Dr. Yiorgos Apidianakis for participating in my examination committee.

I would like to thank my mentor, the PhD candidate Adonis Hajdigeorgiou, for his consistent guidance and help for all years being a member of the lab. I wish him the best of his life.

Special thanks to the rest of the lab members for their support and making the hours in the lab more fun.

I wish to thank all of my friends for their constant support, for always being there for me.

Finally, I am truly most thankful for my family and my boyfriend. Thank you for your unconditional love, constant support, encouragement and for every sacrifice you have made for me throughout my life.

COMPOSITION OF THE EXAMINATION COMMITTEE

Thesis Supervisor (Examination Committee coordinator): Dr. Paris A. Skourides, Professor

Committee Member: Dr. Chysoula M. Pitsouli, Associate Professor

Committee Member: Dr. Yiorgos Apidianakis, Associate Professor

SEMINAR ANNOUNCEMENT

University of Cyprus
Department of Biological Sciences

Master Research Dissertation in Biomedical Sciences (BIO 830/600)

Student Presentation

Thursday, 30 May 2024 at 08:30
Building Library "Stelios Ioannou", Room LRC 019, Panepistimioupoli Campus

This seminar is open to the public

Alexandra Manoli

Thesis Supervisor: Prof. Paris Skourides

"*InvasiCell* is a physiologically relevant in vitro model for the study of tumor progression and the evaluation of potential cancer medications more accurately than current in vitro assays."

Cancer cases have been constantly increasing over the past few decades, leading it to become the second cause of lethality worldwide, with cancer metastasis being responsible for approximately 90%. of cancer-related deaths. Thus, cancer research is essential to enhance our knowledge of the underlying mechanisms that drive tumor progression and metastasis in order to enable the development of new anti-cancer therapies. However, even though in vivo and in vitro models that are currently used in cancer research have provided valuable information on cancer progression, only a few therapies that show promise in vitro studies eventually prove efficacious in clinical studies. Consequently, several studies emphasize the limitations of in vitro models, which are currently used in cancer research, and highlight the need for the development of new more physiologically relevant in vitro models for the study of tumor progression and evaluating the efficacy of potential new anti-cancer medications. The aim of this study was to examine whether *InvasiCell*, a novel device and associated in vitro assay that were developed in our lab, can be used as a physiologically relevant model to study various aspects of tumor progression, compared to the existing in vitro tools that are currently used in cancer research. Specifically, wound healing assays, Boyden chamber assays, *InvasiCell*, and tumor spheroids, were used to evaluate the in vitro invasive potential of previously characterized breast and pancreatic cancer cell lines with known in vivo metastatic potential. The collective data from this study suggest that *InvasiCell* reflects the in vivo metastatic potential of the evaluated cell lines more accurately and reliably than other assays. Additionally, given that fibroblasts are the most abundant stromal cell type in the tumor microenvironment and their role in tumor progression is controversial, we used *InvasiCell* to examine whether the presence of NIH3T3 fibroblasts could affect tumor cell invasive capacity and potentially improve our ability to predict the metastatic potential of tumor cells. Our findings indicate that the inclusion of fibroblasts with cancer cells reduces the invasion potential of various breast cancer cell lines tested. Finally, to examine if *InvasiCell* could be used as a drug response assay, we treated breast cancer cell lines with previously established concentrations of Doxorubicin Hydrochloride under normal tissue conditions or within *InvasiCell*. We observed that the cells within *InvasiCell* displayed enhanced drug resistance, which resembles previously published studies performed with spheroid assays. Collectively, *InvasiCell* can effectively distinguish cell lines with different metastatic capacities, allow researchers to examine tumor cell behavior and interactions by performing co-culture experiments with other cell types, and study cellular resistance to various drugs. Therefore, *InvasiCell* is a promising tool for cancer research, which could enhance our knowledge and understanding of critical steps in tumor progression and facilitate the development of more effective anti-cancer strategies and therapies.

TABLE OF CONTENTS

INTRODUCTION

6.1 Cancer:

Cancer is a significant worldwide health threat since its consistent increase in cases over the past few decades, leading it to become the second leading cause of death (WHO). It is a category of diseases characterized by cell's uncontrolled proliferation and spreading to other parts of the body (Pecorino, 2016). There have been reported more than 200 distinct cancer types, however, the cell type of origin can classify cancer into 5 classes. Carcinoma starts in the skin or from epithelium tissue while sarcoma arises in connective tissues. In addition, leukemia refers to the cancer of white blood cells that starts in the bone marrow where these cells are generated, however, carcinogenesis initiates in immune system cells are called lymphomas and myelomas. Finally, cancers that occur in the central nervous system are categorized as brain and spinal cord cancers (Cancer research, UK).

However, carcinoma is the most frequent category of cancer and represents 80 to 90% of all cancer cases (National Cancer Institute, Cancer Classification). The abnormal epithelial cells proliferate uncontrollably and form an adherent cellular mass of tumor cells. Some of the most common sites where solid tumors are developed are breast, lung, and prostate (Thermo Fisher Scientific, Solid tumor research). Studies demonstrated that the surrounding environment of a solid tumor dramatically affects the tumor growth and progression (Kim, 2022).

6.1.1 Transformation of normal cells to cancer cells:

Genetic alterations such as mutations and epigenetic changes are essential to transform a normal cell into a malignant cell. Specifically, the accumulation of genetic alterations in normal cells contributes to the earlier stage of cancer development (Warenius, 2023). It is known that several factors can cause genetic modifications endogenously and exogenously. Endogenous factors include DNA replication errors and inherent genetic mutations whereas environmental factors such as radiation exposure, lifestyle choices like smoking, and viral infections are some exogenous parameters (Lutz, 1996).

Mutations contribute to cells acquiring a growth advantage when occurring in crucial genes that control cell cycle, DNA repair, apoptosis, and other important cellular processes. Hanahan and Weinberg described six acquired biological characteristics of tumor cells as "hallmarks of cancer" that allow malignant cells to grow and spread. This model comprises autonomous growth signaling, resistance to growth suppressor signals, evading apoptosis, continuous replications, promoting angiogenesis, and induction of invasion and metastasis, as shown in **Figure 1** (Weinberg, 2000). Additional traits of malignant cells include altered metabolism, genomic instability, immune escape, promote inflammation, and epigenetic changes (Douglas Hanahan1, 2011). Therefore, understanding the "hallmarks of cancer" is essential for the development of specialized therapies targeting specific characteristics and molecular pathways, which could improve patients' prognosis and survival. It is known that all these acquired characteristics of malignant cells worsen tumor prognosis and patient survival by increasing metastasis.

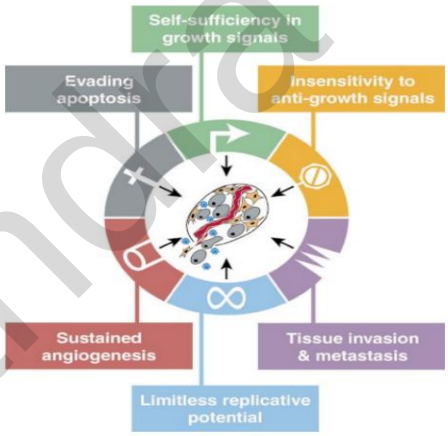

Figure 1: The hallmark of cancers. Cancer cells obtain these six traits to support their continuous growth and dissemination. For instance, tumor cells are sufficient for self-renewal as they secrete growth signal molecules that stimulate their continuous proliferation. Additionally, tumor cells evade growth suppressor signals and resist programmed cell deaths, allowing them to survive and accumulate genetic mutations. Another hallmark of cancer cells is the limitless replicative capacity by maintaining their telomere. Moreover, tumor cells promote angiogenesis to supply the tumor with nutrients and oxygen for further tumor development. Lastly, cancer cells invade the surrounding tissue and then metastasize to distant sites, responsible for the most cancer-related deaths. Adapted from (Hanahan and Weinberg, 2000)

6.2 Metastasis:

Metastasis is defined as the process where tumor cells disseminate from the primary tumor to the distant parts of the body through blood and lymph vessels (National Cancer Institute, Metastatic cancer). It represents the primary cause of lethality for approximately 90% of cancer patients (Lambert, 2017). The metastatic cascade refers to a series of events necessary for metastasis to occur as shown in **Figure 2**. The first steps of metastasis are the local cancer cell spreading and invasion from the original tumor into the surrounding tissue. Following, malignant cells enter the blood or lymph vessels with a process known as intravasation and spread through the body using circulation. After that, tumor cells must persist in the circulation until exit from the vessels through extravasation. Finally, tumor cells must adapt and survive within the environment of the new tissue, activating their division program to establish secondary tumors at those sites (Hapach, 2019).

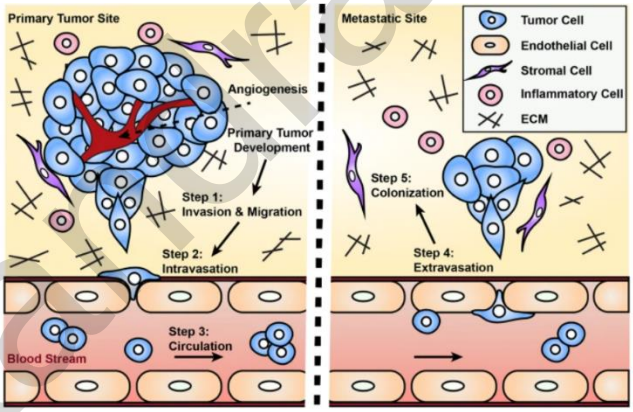

Figure 2: Overview of the metastatic cascade. Metastasis includes a series of sequential steps which are known as tumor metastatic cascade. After the formation of the primary tumor, cancer cells invade the surrounding tissue (invasion and migration) until they encounter blood vessels. The cancer cells enter the bloodstream with a process known as intravasation. Cancer cells have to survive while they travel systemically until they reach a distant organ. At this stage, cancer cells exit from circulation (extravasation) and they need to adapt, survive, and proliferate to establish the secondary tumor at the distant sites (colonization). Adapted from (Hapach et. al, 2019).

Malignant cells potentially can spread to nearly any part of the human body, although specific types of malignant cells tend to metastasize in certain areas (National Cancer Institute, Metastatic cancer). For example, breast cancer, one of the most frequent cancers in women, appears to metastasize prevalently in bone, liver, and lungs (World Cancer Research Fund International, Breast Cancer Statistics). Metastasis in critical sites such as the lungs, brain, and lymph nodes are correlated with poor prognosis and reduced patient survival, however, several studies demonstrate that the specific locations and the number of metastatic tumors are associated with the survival of the patients (Riihimäki 2014, Oh 2009, Tie 2023). Several mechanisms of cell migration including single cell migration and collective migration have been shown to significantly contribute to metastasis.

6.2.1 Single-cell migration:

Epithelial cells can separate from epithelial tissues and gain mesenchymal or amoeboid morphology and characteristics to move as single cells. Epithelial to mesenchymal transition (EMT), mesenchymal to amoeboid transition (MAT), and collective to amoeboid transition (CAT) are three mechanisms that have been described through the conversion of cells' morphology and characteristics (Gandaglia, 2015).

EMT has been described during embryonic development, chronic inflammation, and cancer cell invasion. It has been characterized as an essential procedure for tumor invasion and metastasis (van Zijl, 2011). The distinctive trait of EMT is the reduction of expression of the E-Cadherin which is a transmembrane protein that mediates cell-to-cell interactions (Kalluri 2009, Kaszak 2020). Several factors have been identified to activate intracellular pathways that eventually lead to the reduction of the expression of E-cadherin and obtain mesenchymal characteristics such as the expression of N-cadherin (Cao, 2019). This shift in the expression from E to N cadherin enables the increase in single-cell motility and invasiveness exhibiting a more aggressive phenotype (Peinado, 2007). Additionally, mesenchymal cells are elongated and form membrane protrusions such as lamellipodia and filopodia. Their movement is conducted by the dynamic assembly and disassembly of focal adhesions which mediate the interaction between cell and ECM. Specifically, cells release matrix metalloproteases at their leading edge which degrades the

ECM barrier and allows the movement of the cells (Mrozik, 2018). However, studies have shown that EMT can be reversible, depending on the stage of the metastatic cascade. Mesenchymal to epithelial transition (MET) is crucial for the latest step of the metastatic process. During MET, cancer cells acquire epithelial characteristics and orientation, resulting in the formation of adherent junctions necessary for the establishment of secondary tumors (Yamazaki, 2005).

Despite the mesenchymal phenotype, cancer cells can obtain amoeboid traits to enhance individual cell movement and undergo MAT or CAT. Amoeboid cells have rounded cell morphology and do not display cell polarity and strong interactions with the ECM. Amoeboid cells change their shape by expansion and contraction mediated through actomyosin contractility, resulting in high-speed cell migration (Mrozik 2018, Christiansen 2006).

Thus, cancer cells exhibit plasticity during cell migration and adapt different cell-type phenotype and morphology. Tumor microenvironment, molecular pathways such as RHO/ROCK signaling, and interactions with ECM are some of the factors that induce the switch in migration modes of malignant cells (Santiago-Medina, 2016).

6.2.2 Collective cell migration:

On the other hand, cells can move as a group of connected cells a process known as collective cell migration. This process is observed during embryonic development, tissue regeneration, cancer cell invasion, and metastasis (Wu, 2021). The cluster of cells that undergo collective cell migration consists of two distinct cell populations described as “leader” and “follower” cells. These two cell groups exhibit different topologies and roles to coordinate the synchronized and unidirectional movement of the cellular mass (Friedl, 2009).

Leader cells are localized at the leading edge of the cluster while the dominant follower cells are found behind the leader cells. The direction of migration is provided by leader cells that receive environmental signals. Additionally, polarized leader cells display “finger-like” structures and protrusions such as lamellipodia and filopodia towards the migration direction (Qin, 2021). At the leading side of the leader cell, they form focal adhesion junctions while at the trailing edge, they display adherent interactions with the follower cells. This asymmetric distribution of

connections at the two sides of the cell enables the activation of different molecular pathways (Gov, 2007). For instance, leader cells release signaling molecules such as growth factors and chemokines to guide movement orientation (Malinova, 2018). Furthermore, leader cells secrete ECM remodeling factors to create paths for cell migration (Chapnick, 2014). In contrast, at the rear side of leader cells, cell-to-cell interactions are involved in pathways that maintain the protrusion polarization of the leader cells by inhibiting cell extension and contributing to the coherent migration of cells (Friedl, 2009).

Follower cells have been underestimated for the past year and were described as passengers during collective cell migration. However, studies have demonstrated that the participation of follower cells is crucial and necessary for collective movement (Friedl, 2009). Specifically, the follower cells have been found to generate traction through small "cryptic" protrusions on their basal membrane. Moreover, follower cells facilitate the formation of new leader cells (Friedl 2009, Chapnick 2014, Vishwakarma 2018). Thus, the active contribution of both leader and follower cells is essential for the mechanism of collective cell migration to occur.

Collective cell migration mechanisms have been described in many cancers such as breast, lung, and prostate cancers (Campanale, 2023). Additionally, several studies suggested that collective cell migration exhibits increased invasive potential and therapy resistance compared to single-cell migration (Krakhmal, 2015).

6.3 The tumor microenvironment

Numerous studies have demonstrated that the tumor microenvironment is crucial in tumor growth, local cell invasion, angiogenesis, metastasis, and drug resistance (Yang, 2019). Tumor microenvironment refers to the complex interactions of cancer cells with other cellular and non-cellular components that reside in the surrounding tissue of the tumor. It comprises of a heterogeneous cell population originating from the host along the cancer cells such as fibroblast, endothelial cells, pericytes, and macrophages. Additionally, cancer cells interact with extracellular matrix components like collagen, fibronectin, elastin, and laminin that encompass the malignant cells. The intricate network of communications that exists in the tumor microenvironment causes alteration in cell behavior and morphology (Anderson, 2020).

Intercellular communication among the direct cell-to-cell interactions is mediated by several released molecules including cytokines, chemokines, growth signals, and inflammatory mediators (Baghban, 2020). Lately, studies have illustrated that exosomes, microRNAs, and cell-free DNA are significant for cellular communications, transporting genetic information, and regulating gene expression (Yang 2019, Xiao 2021). All the vital mediators of interactions present in the tumor microenvironment stem from both tumor cells and stromal cells leading to the complexity of understanding these bidirectional interactions (da Cunha, 2019). **Figure 3** in a schematic representation of key components and mediators of interaction that exist in the tumor environment.

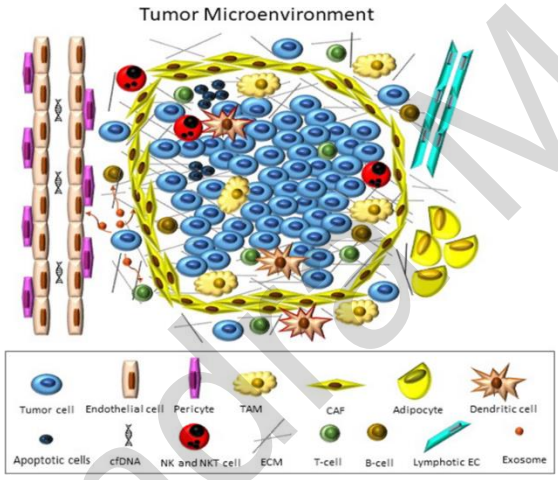

Figure 3: Schematic representation of the tumor microenvironment. The tumor microenvironment is characterized by a heterogeneous cell population. Apart from cancer cells, it includes endothelial cells, pericytes, fibroblasts (CAF), adipocytes, and various immune cells such as dendritic cells, NK cells, T-cells, B-cells, and macrophages (TAM). The interactions between the cells in the tumor microenvironment can be mediated by contact-dependent pathways using soluble factors and ECM components. Furthermore, the cells can interact using horizontal transfer through cfDNA, apoptotic bodies, and exosomes. Adapted from (Baghban et al., 2020)

6.3.1 Physical and biochemical characteristics of the tumor microenvironment

In addition to the several signaling molecules existing in the tumor microenvironment that mediate cellular communication and interactions of cells with ECM components, the tumor microenvironment displays additional characteristics. These properties of the surrounding environment of cancer are vital for tumor survival, growth, immune evasion, and therapy resistance (Pernot 2022,Spill 2016, Kim 2022).

Hypoxia is one of the key features of solid tumors and it can be described as insufficient oxygen supplies to cells due to the constant proliferation and growth of cancer cells. In a tumor microenvironment, oxygen concentrations generate a gradient, and in areas that are proximal to the blood vessels, the oxygen is abundant compared to distant sides (Cairns, 2006). Consequently, at the most hypoxic sites, cancer cells delay their cell division rates or are driven to cell death and form the necrotic core (Li, 2021). Alternatively, cancer cells can acquire adaptations by activating mechanisms that allow them to survive, proliferate, and metastasize despite the low oxygen levels. One key mediator for cellular responses under hypoxia is the hypoxia-inducible factors (HIFs) that include three different proteins 1, 2, and 3 each of which contains two subunits α and β (Mehrabi, 2018). During normal conditions, HIF-1α is degraded, although, under hypoxic environment, HIF-α receives modifications, becomes a dimer with the β subunit, and interacts with other activating proteins (Lee, 2004). As a result, HIFs regulates the transcription of hypoxia-inducible genes that are associated with cell viability, metabolism, and angiogenesis (Suresh, 2023).

Acidosis is an additional characteristic of the cancer's surrounding environment. Studies have shown that the pH in normal tissues is approximately 7.4 however in cancerous tissues it can reach the range of 6.5 to 6.9 (Zhao, 2015). Malignant cells develop multiple mechanisms that contribute to the reduction of the pH in the tumor microenvironment. Otto Warburg has demonstrated that cancer cells shift to aerobic metabolism independently of oxygen concentrations (Estrella, 2013). Under physiological conditions, cells catalyze the glycose and produce two molecules of pyruvate and adenosine triphosphate (ATP) through glycolysis which takes place in the cytoplasm. Followed by oxidative phosphorylation in mitochondria which provides the cell with ATP to utilize for cellular typical biochemical activities (Bensinger, 2012). The Warburg effect demonstrates that cancer cells choose glycolysis as their main energetic

process and convert pyruvate into lactate promoting acidosis in the tumor microenvironment (Estrella 2013, Rigoulet 2020). Furthermore, among other factors, HIF-1a regulates enzymes associated with aerobic metabolism which are necessary for the Warburg effect of cancer cells (Vaupel, 2021). Recent studies have indicated that the acidic conditions of the tumor microenvironment not only affect cancer cells but also contribute to the tumor-promoting functions of non-cancer cells. For instance, malignant cells benefit their cell proliferation, survival, and dissemination. On the other hand, cells surrounding the cancer cells enhance the tumor-promoting effects by alternating their gene expression profiles influenced by acidic conditions (Courtnay, 2015). Overall, acidosis in the tumor microenvironment is linked to several aspects of tumor-promoting processes such as cell migration and invasion, immune evasion, and therapy resistance (Andreucci, 2023).

Recently, several studies focused on elevated interstitial fluid pressure and solid stress in tumors relative to normal tissues (Pillai, 2019). The interstitial space refers to connective and supporting tissues that are located surrounding the parenchymal cells, blood, and lymph vessels. It comprises the interstitial fluid and ECM components. Typically, interstitial fluid is responsible for carrying nutrients and waste products between cells and blood vessels. Moreover, it transports ions, gases, and a variety of signaling molecules such as cytokines between the cells. Thus, interstitial fluid has a significant impact on tissue homeostasis, cellular communication, and immune response (Cairns, 2006). Multiple factors have been demonstrated to raise the interstitial fluid pressure observed in the tumor microenvironment. For instance, cancer cells and stromal cells release molecules that activate fibroblasts and infiltrate immune cells surrounding tumors and as a result, increase the cellular density. Additionally, these stromal cells alter the composition of ECM and promote angiogenesis, leading to a “reactive stroma” (Wiig, 2012). Furthermore, tumors frequently have abnormal leaky blood vessels with increased permeability due to the expression of VEGF. This leads to an increased release of proteins and molecules in tumor mass, resulting in an elevated colloid osmotic pressure of interstitial space. Also, it has been shown that malignancies disturb the flow of lymph within the tumor, consequently impairing the removal of interstitial fluid from the tumor site and increasing pressure in the interstitial space. Collectively, elevated interstitial fluid pressure and solid stress are essential traits of mechanical environment that apply forces and pressure to solid tumors. Studies

demonstrated that these physical forces within the tumor microenvironment significantly affect the effectiveness of cancer therapies and correlate with lymph node metastasis (Wiig, 2010).

6.3.2 Tumor-associated macrophages

Macrophages are immune cells that eliminate pathogens in innate immunity using phagocytosis and contribute to tissue homeostasis by secreting chemokines that recruit other cell types at damaged sites (Heldin, 2004). In the surrounding site of the tumor, distinct types of the host's immune cells are infiltrated, and macrophages are the most extensive immune cells present at these sites. These cells are defined as tumor-associated macrophages and can be distinguished into groups with different functionalities. The role of TAMs is diverse depending on the stage of cancer progression and signals from the tumor microenvironment. It has been demonstrated that tumor-associated macrophages are present at various stages of tumor development and dissemination including secondary tumor sites (Hirayama, 2017).

The M1 macrophages promote inflammation by secreting pro-inflammatory chemokines and reactive oxygen species resulting in the recruitment of other immune cells that attack tumor cells. Although M2 macrophages display support for tumor growth and metastasis through the secretion of chemokines that suppress inflammation and matrix metalloproteinases that disrupt extracellular matrix components contribute to the tumor cell migration and invasion. Additionally, there is a group of M2 macrophages that facilitates angiogenesis due to the combinatory release of chemokines that stimuli endothelial cells to proliferate, change the ECM components, and supply vascularization such as BFGF, VEGF, IL-1, IL-8, TNF-α, MMP-9, and MMP-2 (Bied 2023, Pan 2020). Another important category of macrophages that exists in tumors is metastasis-associated macrophages which support cancer cells in the whole stages of the metastatic cascade. Particularly, studies indicate that macrophages contribute to the entry, surveillance, and exit of malignant cells into the bloodstream and prepare the secondary side for the establishment of metastatic foci (Lendeckel, 2022).

6.3.3 Cancer-associated fibroblasts

Cancer-associated fibroblasts represent another type of stromal cells and are the most abundant in the tumor microenvironment (Lin, 2019). Fibroblasts are in connective tissues and mediate the secretion of ECM components. During wound healing and fibrosis of various organs, fibroblasts become activated and convert to myofibroblasts (Cirri, 2011). This type of fibroblast obtains contractile stress fiber and exhibits the characteristics expression of α-smooth muscle actin (α -SMA) and the ED-A splice variant of fibronectin. It has been observed that CAFs display these traits of myofibroblasts in many tumors. However, unlike myofibroblasts, CAFs are not driven to apoptosis and their activation is irreversible. In addition to the expression of α -SMA, fibroblast specific protein (FSP) and platelet-derived growth factor (PDGF) receptors- β are considered as CAF markers (Lin, 2019).

Several studies have shown that CAFs within the tumor microenvironment can originate from various precursor cells. The primary source of CAFs is the resting fibroblast and stellate cells that are present at the tumor sites. For instance, cancer cells release chemokines and cytokines which activate molecular pathways of resident cells, eventually inducing their transformation into CAFs. Moreover, CAFs can arise from other epithelial or endothelial cells via the mechanisms of epithelial/endothelial-to-mesenchymal transition (EMT/EndMT) respectively. Furthermore, bone marrow recruits mesenchymal stem cells and immune cells such as macrophages in the tumor microenvironment which can be converted to CAFs. It is demonstrated that TGF-β, WNT, and IL-6/STAT3 signaling are important for the transformation of mesenchymal stem cells into CAFs (Hinz, 2007). Therefore, the heterogeneous origin of CAFs contributes to the existence of various CAFs subtypes in the tumor microenvironment with diverse gene expression profiles (Yang, 2023).

Despite the diverse origins and gene expression patterns of CAFs that categorize them in different subpopulations, CAFs display conflicting functions with tumor-promoting and tumor-suppressive roles in the tumor microenvironment. Particularly, it is evident that CAFs support tumor development by the secretion of pro-inflammatory, immune-suppressive, ECM remodeling, and angiogenesis factors. However, other studies revealed some tumor-suppressive functions of CAFs. For example, CAFs were shown to eliminate the invasion and self-renewal of

cancer stem cells and delay tumor progression by enhancing the sensitivity to the treatment (Weber, 2009).

The development of new anti-cancer therapies targeting stromal cells, particularly CAFs, has been rapidly growing. Due to the understanding of the presence of varying CAFs subtypes with different functionalities, new therapies must focus on targeting those that display tumor-promoting effects (Feng, 2022). Some of the existing approaches include the blocking of the differentiation of CAFs from other cells and the selective depletion of CAFs tumor-supportive populations. Other strategies involve reprogramming the tumor-promoting CAFs into tumor-suppressive CAFs and inhibiting the interactions between cancer cells and CAFs to diminish their tumor-promoting function (Hinz, 2007). All these approaches for targeting tumor-supportive CAFs are schematically summarized in **Figure 4**.

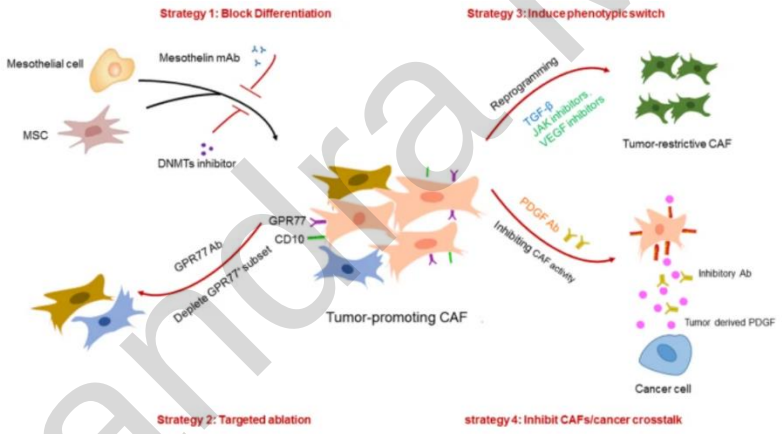

Figure 4: Current approaches for selectively targeting tumor-promoting CAFs in the tumor microenvironment. The first approach aims to block the differentiation of other cell types such as mesenchymal or mesenchymal stem cells into CAFs by inhibiting of signaling pathways responsible for that. The second approach is to use genetic manipulation tools or antibodies to target specifically only the tumor-supportive CAFs populations. Thirdly, scientists promote the differentiation of tumor-suppressive CAFs by inducing reprogramming of tumor-supportive to acquire phenotypes of the suppressive populations. Finally, specific antibodies block the signaling molecules that are important for cancer cells and CAFs interactions resulting in the inhibition of the CAFs function. (Adapted from Yang et al, 2023)

6.4 *In vivo* and *in vitro* tools for cancer research:

6.4.1 *In vivo* models used in cancer research

In vivo models have a crucial role in cancer research, because using animal models, such as mice, provides the ideal recapitulation of the tumor microenvironment. This is the main advantage of *in vivo* models, as it presents the greatest challenge of *in vitro* models (Chen, 2019). Mice and rats are the most favored animals in cancer research due to being closely related to humans and the extensive knowledge about their genetic background (Katt, 2016). Specifically, mouse models have been used to examine fundamental processes for tumor progression like metastasis and drug resistance. Furthermore, they are considered pre-clinical models for the evaluation of anti-cancer treatments. Moreover, genetically engineered and immunocompromised mice are used for tumor xenografts to examine primary and metastatic tumor growth (Chandra, 2020). However, *in vivo* models come with limitations, thus the utilization of *in vitro* tools in cancer research is a necessity. For instance, working with animals comes with ethical concerns, is costly, time-consuming, labor-intensive due to the demands of special researchers and laboratory facilities (Martinez-Pacheco, 2021), and usually can only provide end point evaluations.

6.4.2 Commonly used *in vitro* models for cancer research:

In vitro tools have the advantages of being efficient, easily controlled, low cost, and provide easily reproducible experiments related to *in vivo* models (Jubelin, 2022). Several *in vitro* tools are used in cancer research and each of them is utilized to examine different stages of cancer cell development and dissemination. Thus, *in vitro* models can be classified into different levels of complexity, ranging from 2D to 3D models (Chen, 2019).

6.4.2.1 Wound healing assays:

Wound healing assays, also known as scratch assays, are widely used in cancer research, and considered as essential 2D *in vitro* tools for research. Wound healing is a cellular process responsible for tissue regeneration after injury or damage under physiological conditions (Grada,

2017). These assays are applied to study collective cell migration and multiple studies have utilized them to examine the migration capacity of malignant and non-malignant cells under different experimental conditions (Christensen 2013, Migliaccio 2023, Ahmadiankia 2016). Specifically, scientists generate a scratch in a confluent monolayer of cells using a pipette tip for example, and the migration of cells is estimated by the gap closure over time. The exact procedure of wound healing assays is shown in **Figure 5.** Additionally, they mentioned that to minimize the contribution of the proliferation factor to the closure of the gap, they usually conduct wound healing assays for a short time from 8-24 hours and use starvation media without growth factors. Thus, these assays are quick, simple without the necessity of any special equipment, adaptable, and cost-effective (Christensen 2013, Migliaccio 2023).

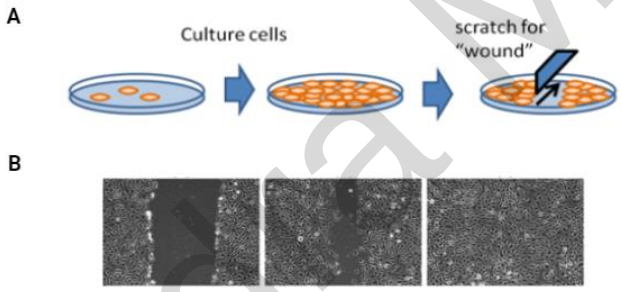

Figure 5: Wound healing assay for studying migration abilities of cells. (A) The wound healing assay is conducted on a confluent monolayer of cells by generating a scratch using a pipette tip. **(B)** The migration ability of cells is assessed by observing the gap closure over time. Adapted from (Bise et a, 2011)

6.4.2.2 Boyden chamber assays:

The most commonly used 2D *in vitro* assay for examining tumor cell invasion is the transwell migration assay, also called Boyden chamber assay. The main concept of these assays is based on a porous membrane where the cells migrate through the pores which can vary between 3-12μm diameter. Specifically, the membrane insert generates the two-chamber system consisting

of the upper and the lower (Bise, 2011). The cells are seeded on the upper chamber in a serum-free medium and then migrate through the porous into the lower chamber which comprises a full serum medium or chemoattractant as shown in **Figure 6.** The migration ability of cells is determined by the number of cells that move to the lower chamber relative to the initial cell population (Schirmer, 2024). Thus, transwell migration assays are effortlessly implemented (Katt, 2016).

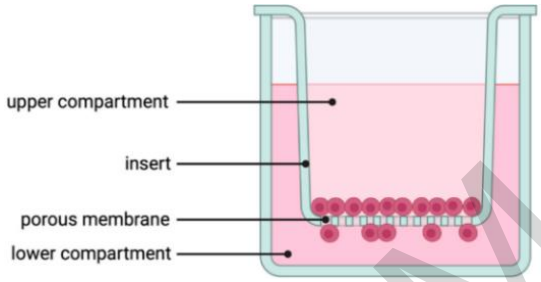

Figure 6: Schematic representation of the Boyden chamber assays that are used to examine cell migration. The insert membrane creates a two-chamber system, the upper chamber and the lower chamber. The examining cells are placed in the upper chamber in a serum-free media whereas the lower chamber consists of full-serum media. The migration ability of the cells is estimated by the number of cells compared to the initial cell population that migrate through the porous membrane into the lower chamber. Adapted from (Schirmer et al., 2024).

6.4.2.3 Modified Boyden chamber assays:

Although these 2D *in vitro* assays are considered by many researchers to be unreliable self-sufficient pre-clinical models for cancer research. Primarily, both wound healing and transwell migration assays are excessively basic and display low physiological relevance. Particularly, the lack of essential players in the tumor microenvironment such as ECM components and other cell types can alter the cell's capacities including the migratory abilities, shape, and intracellular pathways as mentioned before (Kramer, 2013). Therefore, there was a need to develop *in vitro* models with increased complexity to better mimic the *in vivo* microenvironment. An approach to achieve that is the inclusion of ECM components and other cell types in these assays. For

example, scientists used modified transwell assays by including ECM like Matrigel or collagen. Particularly, the membrane insert which generates the two-chamber system is coated with an ECM component. Then, cells are seeded on the upper chamber in a serum-free medium, invade through the ECM barrier and pass via the porous membrane into the lower chamber which consists of full serum medium, as shown in **Figure 7**. Through this approach, they evaluate the invasion capacity of cells, defined as the movement of cells in a 3D environment and the remodeling of ECM (Schirmer 2024, Justus 2023). Even with the presence of ECM and co-cultures with other cell types which results in more realistic morphology of cells compared to 2D *in vitro* models, these techniques are characterized as 2.5D. This is due to cell-to-cell and cell-to-ECM interactions occurring only at the side of contact instead of the entire 3D environment as existing in a living organism condition (Zhang 2017, Shamir 2014).

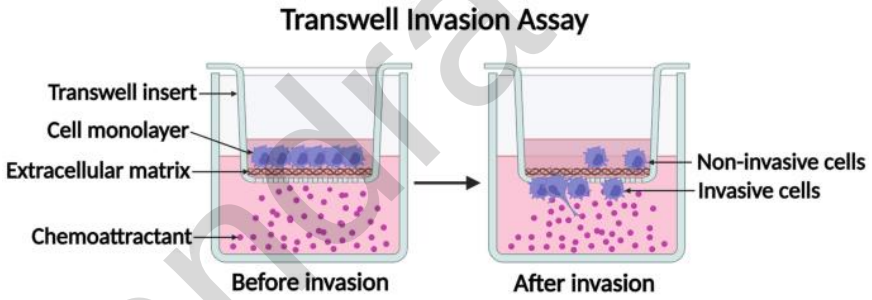

Figure 7: Schematic representation of the Modified Boyden chamber assays for examining invasive abilities of cells. The porous membrane of the insert is coated with an extracellular matrix component such as Matrigel or collagen. The examining cells are placed on the upper chamber in a serum-free media whereas the lower chamber consists of full-serum media. The invasion ability of the cells is estimated by the number of cells compared to the initial cell population that invade through the ECM barrier and pass via the porous membrane into the lower chamber. Adapted from (Justus et al., 2023).

6.4.2.4 Tumor spheroid-based assays:

Currently, many scientists are increasingly focusing on 3D *in vitro* tools for cancer research. 3D *in vitro* models are intricate relative to 2D models however, they mimic crucial aspects of the tumor microenvironment. Under the pressure of the tumor microenvironment, tumor cells can preserve their tumorigenic characteristics which can support the investigation mechanisms responsible for cancer progression, metastasis, and drug development using an *in vitro* tool (Tidwell, 2021). Tumor-spheroids assays are the gold standard 3D *in vitro* models to study tumorigenesis, metastasis, and drug screening. Cancer spheroids are aggregates of cells that can be formed by several methods. This can occur through an anchorage-independent system where cells are in suspension or through an anchorage-dependent system where cells are embedded into ECM, as illustrated in **Figure 8** (Katt 2016, Manduca 2023). Thus, tumor spheroid-based techniques mimic and allow the examination of cell-to-cell and cell-to-ECM crosstalk that are present in living organisms. The size of spheroids can vary, yet those exceeding 200μm can establish oxygen and nutrient gradients which are additional elements of the tumor microenvironment that can be replicated in spheroid-based assays. Also, a necrotic core and an external proliferative zone with dividing cells that resemble a solid tumor can be generated with even larger spheroids beyond 500 μm (Langhans, 2018). Moreover, spheroids can be created by co-culturing different cell types such as fibroblasts which enables the study of interactions between these cell types in cancer progression. Furthermore, scientists demonstrate that this co-culture system effectively replicates the EMT process and local cell invasion observed at early stages of metastasis *in vivo* (Zanoni, 2016). Despite the advanced representation of the 3D environment of tumors, spheroid-based assays have limitations. Firstly, it is shown that the lack of uniformity in size and density of tumor spheroids across multiple experiments significantly can affect the examining parameters like drug response leading to low reproducibility (Kim, 2015). Secondly, the generation of tumor spheroids can be challenging and time-consuming due to cell lines like the breast cancer MDA MB-231, which cannot form tightly adherent spheroids (Gong, 2015). Therefore, these assays are unsuitable for high-throughput drug screening (Kim, 2015).

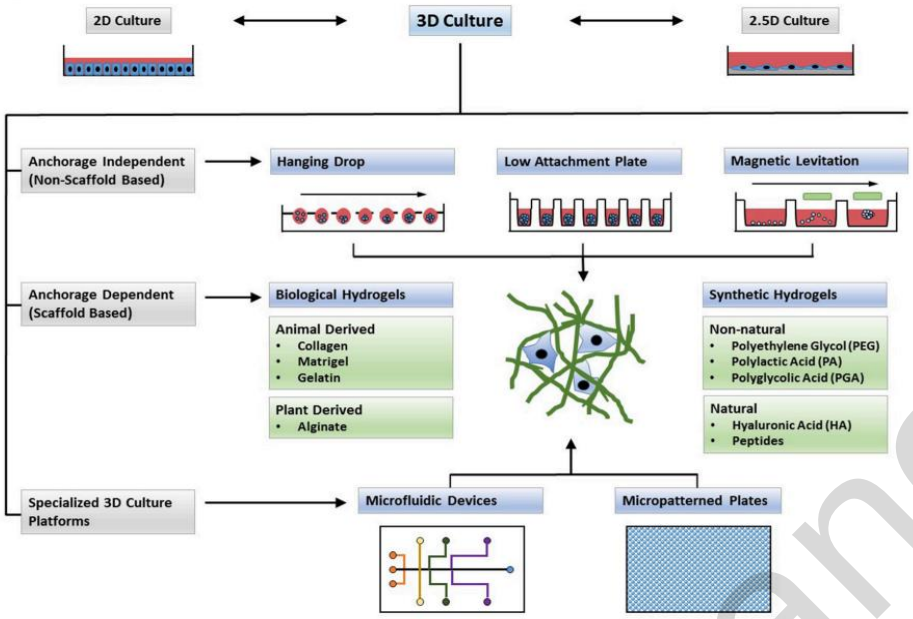

Figure 8: Schematic representation of the different techniques that are used to generate 3D culture spheroids. Anchorage-independent methods include hanging drop, low attachment plate, and magnetic levitation where the cells are in suspension, and these approaches allow cells to generate aggregates. On the other hand, cells can be embedded in biological or synthetic hydrogels and assist the formation of 3D spheroids, which are categorized in anchorage-dependent methods. Additionally, there are more complex approaches such as microfluidic devices and micropatterned plates that are specialized to generate 3D spheroids. Adapted from (Langhans, 2018)

6.4.2.5 Microfluidic devices:

Microfluidic devices are considered promising *in vitro* tools that are used in cancer research. Currently, there exist varying microfluidic-based devices that highly mimic the tumor microenvironment and facilitate the identification of biomarkers that improve the diagnosis and treatment (Han, 2021). In addition, microfluidic devices provide numerous applications that replicate almost every stage of cancer progression and metastasis such as the investigation of cell migration, invasion, immune responses as well as intravasation and extravasation (Katt 2016, Azadi 2020). Furthermore, these tools can be utilized in high throughput drug screening and single-cell analysis enabling the study of cellular heterogeneity within cancer cell populations and enhancing precision medicine (Bargahi, 2022). Despite the significant contribution of microfluidic devices in cancer research, they also have limitations. For instance, the setup of these tools is quite complex, requires user expertise, and is costly due to the need for additional equipment to achieve the high recapitulation of the tumor microenvironment (Azadi 2020, Han

2023). For the above reasons such devices has remained a niche tool with relatively limited use by the research community.

6.5 Generation of *InvasiCell*:

These i*n vitro* models have provided essential information about cancer progression and metastasis, although due to their pre-mentioned limitations have poor *in vivo* translational potential. Studies emphasized the drug efficiency gap between *in vitro* and *in vivo*, since only a few therapies that show promise *in vitro* eventually prove efficacious in clinical studies (Jubelin, 2022, Jardim 2017). Therefore, the development of new more physiological relevant *in vitro* models for studying tumor progression and evaluating the efficacy of drug is required (Mahalmani 2022, Sensi, 2019).

Considering the limitations of the current *in vitro* models and their limited *in vivo* translation, our group (Skourides Lab) developed a novel device called *InvasiCell* which forms the basis for a new *in vitro* assay that can advance the examination of cancer, focusing on tumor invasion and metastasis. *InvasiCell* has a straightforward setup and facilitates quick experimentation. It contains a central circular core which allows the formation of tumor spheroids of every cancer cell line independently from its capacity to generate spheroids. *InvasiCell* can be utilized to study the first steps of the metastatic cascade which are tumor formation and local cell invasion. Particularly, tumor cells are embedded in a low serum collagen gel that imitates ECM and invades through an outer full serum gel. Finally, a full serum media is placed on the device to create a chemoattractant towards the cells and stimulate their invasion. **Figure 9** illustrates a schematic representation of a general setup invasion assay using the *InvasiCell* device.

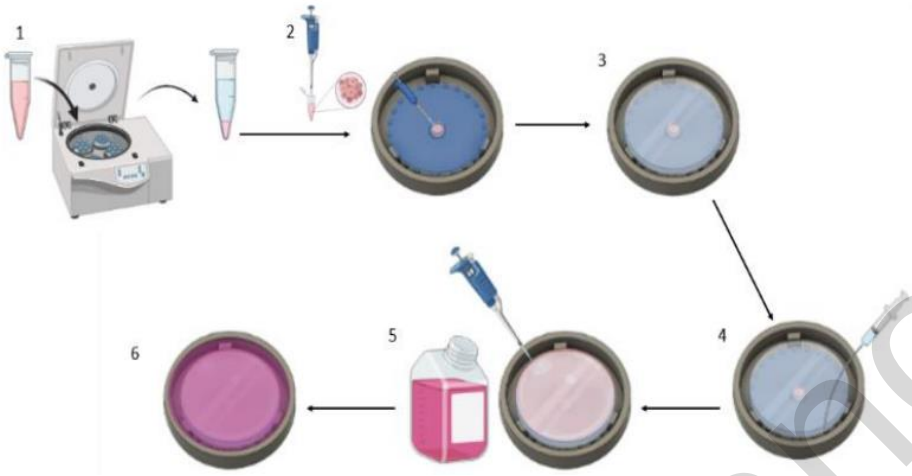

Figure 9: Schematic representation of the InvasiCell devise setup protocol. 1) Sample preparation: Performing a normal passage protocol, cells are harvested and centrifuged for 5 minutes at 1000rpm, followed by the immediate removal of the supernatant. 2) The cells (pellet) are resuspended in the low-serum collagen gel to achieve a concentration of 100.000 cells and 1.5µl of the mixture is immediately introduced in the device's central core. 3) A glass round coverslip is placed on the top of the device, thus sealing the device. The device is then placed in the incubator for 11 minutes until the collagen gel is polymerized. 4) After, a full serum collagen gel that mimics ECM is introduced to the invasion zone of the device through the side and then again placed in the incubator in a humid environment for its polymerization. 5)Finally, the cell culture media, is added to immerse the device. 6) The device is ready for imaging or placement in an incubator for subsequent analysis.

6.6 Characterization of *InvasiCell* device:

Furthermore, according to unpublished data generated by the Ph.D canditate Adonis Hajdigeorgiou, *InvasiCell* recapitulates conditions of the tumor microenvironment present in virtually every solid tumor. Specifically, the collective data have shown that the device can establish de novo stable gradients of nutrients, oxygen, and pH. Moreover, Adonis' showed that the tumor spheroids generated inside *InvasiCell* exhibit the three characteristic regions such as growing solid tumors in living organisms. For instance, the tumor spheroids display a central

necrotic core where cells have died, a periphery ring where the cells undergo apoptosis due to the lack of oxygen and nutrients, and a proliferative ring where cells are actively dividing because of the availability of nutrients and oxygen. All the gradients and the three characteristic rings observed in the tumor microenvironment can be replicated using the *InvasiCell* device, as shown in **Figure 10**. Thus, *InvasiCell* provides the investigation of the invasive potential of various cancer cell lines under conditions that exist in a 3D *in vivo* environment.

A

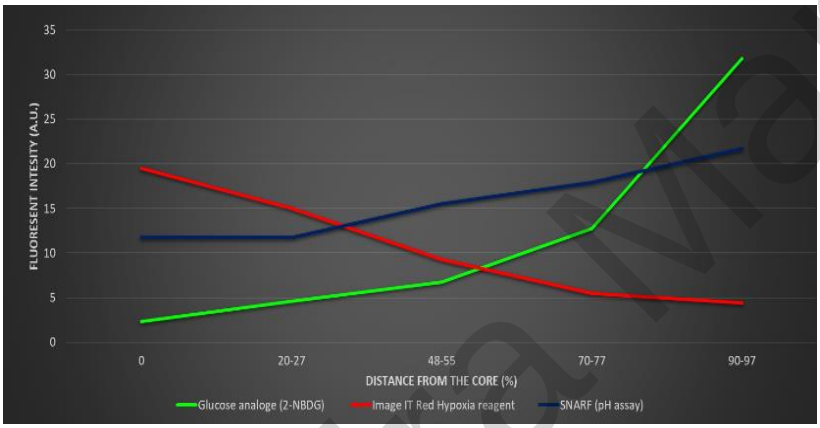

B

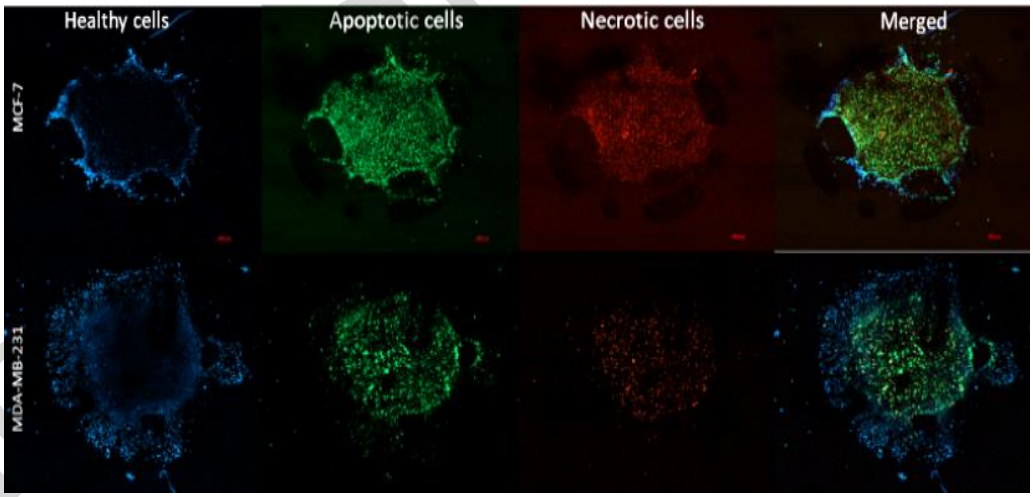

Figure 10: InvasiCell device recapitulates conditions that exist in the tumor microenvironment. A) The *InvasiCell* device generates de novo gradients of nutrients (green), oxygen (red), and acidosis (blue). In the core of the device where tumor cells are placed, conditions such as starvation, hypoxia, and acidosis exist as found in solid tumors. However, as moving away from the core, there is a greater availability of nutrients and oxygen, the pH increases, resembling conditions near the blood vessels in the tumor microenvironment. **B)** MDA and MCF-7 cells were used to set up invasion assays using the *InvasiCell* device, and after 48 hours the devices were stained using a necrosis/apoptosis assay kit. The healthy cells are shown in blue, the apoptotic cells in green, and the dead cells are shown in red. The tumor spheroids generated by the device form a central necrotic core (red), a periphery ring with cells driven to apoptosis (green), and an external ring with healthy cells that are actively proliferating due to the higher availability of nutrients and oxygen in this region. These three characteristic features are observed in solid tumors. (Unpublished data from Adonis Hajdigeorgiou).

6.7 Generation and isolation of MDA-i cell line:

Taking into account that *InvasiCell* recapitulates conditions and induces similar selection pressures that exist in the tumor microenvironment, we proceeded with the isolation of cells after conducting invasion assays using the device. Particularly, the aim of my undergraduate thesis (Alexandra Manoli, 2022) was to examine how the selective pressures applied by *InvasiCell* which mimic the *in vivo* situations, have an impact on the metastatic abilities of cancer cells. Therefore, during my undergraduate project we have isolated the MDA-i cell line from MDA-MB-231 (MDA) cells using *InvasiCell.* Specifically, MDA -GFP stable cells were introduced into the core of the *InvasiCell* device, and those that invaded beyond the invasion zone of the device were isolated. Then the process was repeated by using the MDA P1 (passage 1 from the device) cells, and the cells that exited the invasion zone were re-isolated, resulting in the generation of the MDA-i cell line (passage 2 from the device).

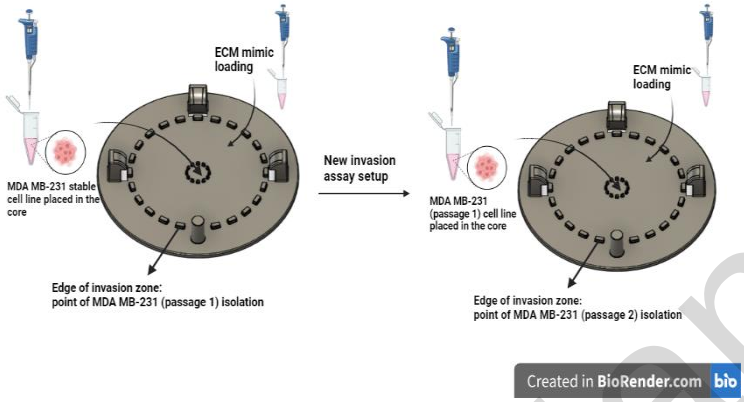

Figure 11: The generation and isolation of MDA-i cell line. MDA stable cells were introduced in the core of device and the ones that exited the invasion zone of the device were isolated. After that, these isolated cells (MDA MB-231-GFP passage 1) were introduced to the device, and the re-isolation led to the generation of the MDA MB-231-GFP (passage 2) cell line.

6.8 Characterization and comparison of isolated MDA-i cell line:

Our objective was to assess any differences between the parental MDA and isolated MDA-i cell lines which can be generated by the applied pressures of the *InvasiCell* which could lead to enhance the metastatic potential of isolated MDA-i cells.

Firstly, we investigated some essential cellular characteristics of cancer cell lines such as proliferation rates and migration abilities. To evaluate the proliferation rates of these cell lines, we used fluorescence intensity as an indicator, and our data revealed that under physiological conditions MDA and MDA-i cell lines showed similar proliferation rates. However, we observed that under conditions that exist in the tumor microenvironment such as starvation, hypoxia, and acidosis MDA-i cells displayed significantly increased proliferation compared to the parental MDA cells. Afterward, we proceeded to investigate the FA kinetics which is crucial for the migration abilities of cells through time-lapse confocal microscopy using paxillin as a focal adhesion marker. Our data showed that the isolated MDA-i cells exhibit faster FA turnover

whereas FAs of the parental cells have a longer lifetime, suggesting that the isolated cell line displays higher migration abilities.

Following that, we investigated whether these two cell lines have gene expression changes that could explain the altered phenotype of isolated MDA-i cells. Thus, we conducted western blot analysis and our data showed that c-Myc which is a known oncogene associated with uncontrolled cell proliferation was remarkably overexpressed in MDA-i cells. Although, p53 which is a tumor suppressor protein, was significantly downregulated in the isolated MDA-i cells compared to their parental MDA cells. Furthermore, the activated phospho-FAK was slightly elevated in the isolated MDA-i cells relative to the parental MDA cells. This could explain the faster FAs disassembly and assembly of MDA-i cells since FAK has a crucial role in the kinetics of FAs.

Finally, to validate the increased proliferation rate under conditions that exist in the tumor microenvironment and the elevated migration abilities of MDA-i cells, we performed in vivo experiments. Orthotopically injection into nude mice revealed that MDA-i cells showed greater tumor establishment ability and formed larger tumors compared to MDA cells. Additionally, the isolated MDA-i cells generated greater number of metastatic foci in the lungs of mice, as shown in **Figure 12**. Therefore, in vivo experiments confirmed the altered phenotype of isolated MDA-i cells observed in vitro relative to parental MDA cells.

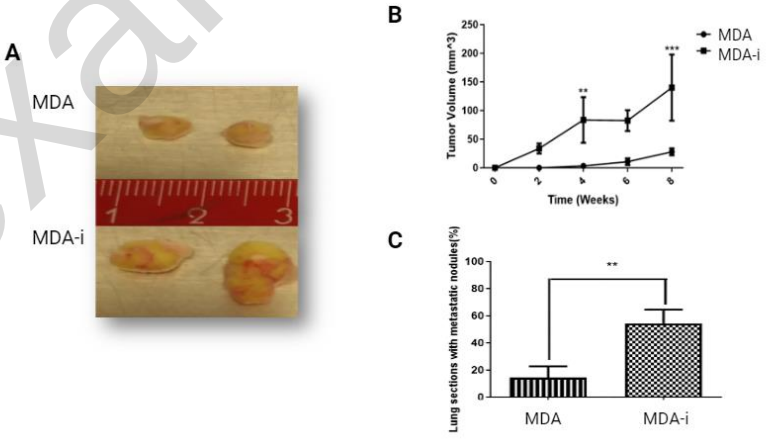

Figure 12: The *in vivo* experiments validated the altered phenotypes of isolated MDA-i cells observed *in vitro*. A) Images of primary tumors from isolation 8 weeks post orthotopic injections. Mice were injected with MDA 3x10^6 cells and their primary tumors (n=2) are present above. Mice were injected with 3x10^6 isolated MDA-i cells, and their primary tumors (n=2) are shown below. Mice injected with the isolated MDA-i cells formed larger tumors than those injected with the parental MDA cells. **B)** The graph illustrates the tumor volume of mice (mm^3) over time (weeks post injections). The data showed that MDA-i cells established tumors earlier and formed larger tumors in mice compared to MDA cells. **C)** The graph shows the percentage of lung sections with metastatic nodules from mice that were injected with MDA and MDA-i cells. Data suggests that MDA-i cells significantly higher number of metastatic foci compared to MDA cells.

6.9 Examining the *InvasiCell* device for the isolation of cells with increased metastatic potential:

Considering all the data from the characterization and the comparison between the parental MDA and the isolated MDA-i cells, Adonis Hajdigeorgiou progressed with the isolation of another cell line. Particularly, he used the pancreatic cancer cell line PANC-1 as parental cells. Following the same procedure used for MDA-i cells isolation, he generated the isolated PANC-i cell line. Unpublished data from our lab suggest that the parental PANC-1 cells displayed higher expression of E cadherin compared to the isolated PANC-i cells. However, the isolated PANC-i cells exhibit increased expression of N-cadherin compared to their parental cells. This data indicates that the isolated PANC-i cells undergo EMT by switching their expression of cadherins while in the device. Studies suggested that the EMT contributes to the migration and survival of cancer cells during initial steps of metastasis (Safa, 2020). In order to evaluate the in vivo metastatic potential of the parental PANC and isolated PANC-i cell lines, Zebrafish xenografts experiments were performed. Data generated by Konstantinos Chatzileris showed that the isolated PANC-i cells exhibited higher incidence of metastasis and dissemination of cells to the tail fin compared to the parental PANC cells (**Figure 13**). Thus, the *InvasiCell* isolated PANC-i cell line displayed greater in vivo metastatic potential than the parental PANC cells.

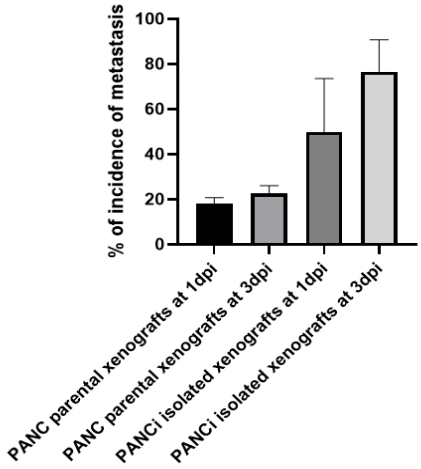

Figure 13*: In vivo* experiments using Zebrafish xenografts validated the higher in vivo metastatic potential of the isolated PANC-i cell line compared to the parental PANC cell line.Cells (PANC and PANC-i) were transplanted in the PVs (Perivitelline space) of 2dpf (2 days post fertilization) zebrafish embryos (n=30 for each cell line). Xenografts injected with the isolated PANC-i cells displayed higher incidence of metastasis both at 1dpi and 3dpi (days post injections). Data generated by Konstantinos Chatzileris

MATERIALS AND METHODS

7.1 Cell lines:

MCF-7, MDA MB 231-GFP stables (generated by Ph. D candidate Maria Christoforou), and MDA MB 231 -GFP isolated, MDA231-LM2-4175, PANC-1, PANC-1 isolated, MIA PaCa-2 and NIH/3T3 cells were cultured at 37°C with 5% CO2 in Dulbecco's Modified Eagle's Medium-DMEM (UltraCruzTM) supplemented with 10% Fetal Bovine Serum (PANTM Biotech) and 1X Antibiotic/Antimycotic solution (Biosera). Trypsin-EDTA 0.05%/0.02% in PBS (PANTM Biotech) and 1XPBS pH 7.4 (Gibco) were used during cell splitting and cell passaging from a confluent 6cm plate (UltraCruzTM). Cells were cryopreserved at a temperature of -194oC in liquid nitrogen with complete growth medium supplemented with 5% (v/v) DMSO (SigmaAldrich).

7.2 Wound healing assays:

Cells were seeded in charged 2-well glass-bottom μ-slide (Ibidi) with DMEM supplemented with 10% FBS and 1X Antibiotic/Antimycotic solution. After the cells reach the confluence, DMEM was substituted by Leibovitz's L-15 Medium (Gibco) supplemented with 1% FBS 1X Antibiotic/Antimycotic. Then, a 200-μl sterile plastic micropipette tip was used for scratch-making in the monolayer of cells to create a cell-free gap. The starvation situation was performed to avoid the proliferation factor of cells affecting the gap closing. Finally, the slides were placed in the ibidi control system, and the temperature was stable at 37°C for live imaging. Live Imaging was performed on a Zeiss Axiovert 200M Microscope with the Axiovision software (AxioVs40 V 4.7.2.0) using 5X magnification with 2-hour intervals for 24 hours.

7.3 Transwell migration assays (Boyden chamber):

All transwell migration experiments were conducted using the 12-well insert 8.0 μm PET clear (cellQART®) for 12-well tissue culture plates (UltraCruzTM). Cells and inserts were subjected to starvation conditions 24 hours prior to the experiments. Cells were seeded in a 6cm plate and after becoming confluent, cells were starved by adding 5 ml of DMEM supplemented with 0.2%

FBS for 24 hours. The inserts were placed in a 12-well plate, where each insert contained 500μl of DMEM supplemented with 0.2% FBS on the upper side for 24 hours. The starvation media was removed from the upper side of inserts and two 200.000 cells were seeded within the upper side of inserts in 500μl of DMEM supplemented with 0.2% FBS. Each well of the 12-well plate containing the inserts was filled with 750μl of DMEM supplemented with 10% FBS 1X Antibiotic/Antimycotic solution to generate a gradient for cell migration. After that, the cells were allowed to migrate through the porous membrane of the insert for 24 hours. Then, all media were aspirated from both the upper and lower sides of the inserts and a cotton swab was used to gently scrapping any remaining cells from the upper side of the inserts membrane. Following, the inserts were placed in 400μl of Trypsin-EDTA 0.05%/0.02% in PBS per well and the 12-well plate was placed in the incubator at 37°C with 5% CO2 for 5 minutes. Subsequently, cell counting was performed and the migration percentage was determined. Migration percentage = number of cells in the lower chamber of insert/ total number of cells seeded in the upper chamber ×100%.

7.4 Modified transwell migration assays:

The upper chamber of the 12-well insert was coated with 100μl of 0.125% collagen gel consisting of 192μl DMEM with 10% FBS and 1X Antibiotic/Antimycotic solution, 11μl 10X PBS (Gibco), 0.313μl NAOH 1M, and 6.69μl Collagen I, rat tail (3-4 mg/ml) (Santa Cruz Biotechnology). Then, the 12-well plate containing the coated inserts was placed in the incubator at 37°C with 5% CO2 for 24 hours. Following, cells and inserts were subjected to starvation conditions 24 hours prior to the experiments. Cells were seeded in a 6cm plate and after becoming confluent, cells were starved by adding 5 ml of DMEM supplemented with 0.2% FBS for 24 hours. The inserts were placed in a 12-well plate, where each insert contained 500μl of DMEM supplemented with 0.2% FBS on the upper side for 24 hours. The starvation media was removed from the upper side of inserts and 500.000 cells were seeded within the upper side of inserts in 500μl of DMEM supplemented with 0.2% FBS. Each well of the 12-well plate containing the inserts was filled with 750μl of DMEM supplemented with 10% FBS to generate a gradient for cell migration. After, the cells were allowed to migrate through the porous membrane of the insert for 48 hours. Afterward, all media and collagen gel were aspirated from

the inserts and a cotton swab was used to gently remove any remaining cells from the upper side of the inserts membrane. Following, the inserts were placed in 750μl of Trypsin-EDTA 0.05%/0.02% in PBS per well and the 12-well plate was placed in the incubator at 37°C with 5% CO2 for 5 minutes. Subsequently, cell counting was performed and the migration percentage was determined.

7.5 Generation of tumor spheroids:

Three-dimensional tumor spheroids were generated using 1% agarose-coated 96-well plate (UltraCruzTM) to prevent cells from to attach the surface. Each spheroid initially consists of 2500 cells and by performing normal cell passage protocol, the relevant volume was placed per well. After the addition of DMEM supplemented with 10% FBS to reach the final volume of 100μl per well, the plate was centrifuged at 1100 rpm, 200g for 5 minutes to form cell aggregates. Subsequently, cell aggregates were allowed to generate spheroids in the incubator at 37°C with 5% CO2 for 48 hours. Following, the media from each well was gently aspirated using a 0.5 ml syringe and then the spheroids were embedded in 100μl an ECM mimic collagen gel. The gel contains 89 μl DMEM supplemented with 10% FBS, 11 μl 10XPBS, 5 μl NAOH 1M, 2 μl Antibiotic/Antimycotic solution, and 107 μl Collagen I. Afterward, the spheroids were placed in the incubator at 37°C with 5% CO2 for 1 hour and a volume of 100 μl of DMEM supplemented with 10%FBS was added per well. Then, to evaluate the invasive potential of different cell lines, static images were obtained for 3 days by using the Zeiss Axiovert 200M Microscope and Axiovision software (AxioVs40 V 4.7.2.0).

7.6 Invasion assay using *InvasiCell* device:

7.6.1 Treatment of the device before the setup of the invasion assay:

The polydimethylsiloxane (PDMS) (Dow Corning) made devices were initially charged by their introduction to a plasma chamber for 3 minutes. Subsequently, the devices were treated with vapor saline for 3 minutes. Additionally, the round 15mm glass coverslip (Thermo Scientific) which is sealing the device, was treated with Rain-X.

7.6.2 Solutions for invasion assay were prepared:

-Inner collagen gel (2%): 64 μl DMEM, 25 μl DMEM supplemented with 10% FBS and 1X Antibiotic/ Antimycotic solution, 11 μl 10X PBS, 5 μl 1M NAOH, 2 μl 1X Antibiotic/Antimycotic solution, and 107 μl Collagen I.

-Outer collagen gel (2%): 89 μl DMEM supplemented with 10% FBS and 1X Antibiotic/Antimycotic solution, 11 μl 10X PBS, 5 μl 1M NAOH, 2 μl 1X Antibiotic/Antimycotic solution and 107 μl Collagen I.

The DMEM supplemented with 10% FBS in the outer gel is a 3:1 ratio with the inner gel to generate a growth factor gradient, which operates as a chemoattractant for the cells.

7.6.3 Sample preparation for invasion assay:

Succeeding a normal passage protocol, 1 ml of cells was collected in an Eppendorf tube and centrifuged for 6 minutes at 1000rpm. After the removal of the supernatant, cells were washed by adding 1ml of 1X PBS and were centrifuged again for 6 minutes at 1000rpm, followed by the disposal of the supernatant. Then the cells were resuspended in the inner collagen gel to achieve a final concentration of 100,000 cells.

In co-culture experiments with fibroblasts (NIH/3T3), following normal passage protocol, 1 ml of NIH/3T3 cells was additionally collected in an Eppendorf tube. Cancer cells and fibroblasts are in a ratio of 5:1 in the inner gel which is placed in the core of the device. The relevant volume of NIH/3T3 cells was added to the Eppendorf containing the cancer cells and centrifuged for 6 minutes at 1000 rpm. After the removal of the supernatant, the mixture of cancer cells and fibroblasts was washed by adding 1ml of 1X PBS and was centrifuged again for 6 minutes at 1000rpm, followed by the disposal of the supernatant. Then the cells were resuspended in the inner collagen gel to achieve a final concentration of 120,000 cells.

7.6.4 The setup of invasion assay using *InvasiCell*:

Immediately after the resuspension of cells in the inner gel, 1,5μl from the mixture was introduced into the device core, which is designed by the inner posts. Then, a round 15mm glass coverslip (Thermo Scientific) was placed on the PDMS outer spacers of the device, converting the droplet into a round disc. Next, for the polymerization of the hydrogel, the device was placed in an incubator at 37°C with 5% CO2 for 11 minutes. Following that, to form the invasion zones of the device, the outer collagen gel solution was introduced around the core of the device until the area designated by the device's outer posts was completely occupied. Subsequently, for the polymerization of the hydrogel, the device was placed in an incubator at 37°C with 5% CO2 for 30 minutes. Finally, DMEM supplemented with 10% FBS and 1% 1X Antibiotic/Antimycotic solution was added until the device was completely immersed. Then, to evaluate the metastatic potential of different cell lines, static images were obtained every day by using the Zeiss Axiovert 200M Microscope and Axiovision software (AxioVs40 V 4.7.2.0) until the cells reached the outer spacers.

7.7 Immunostaining on invasion assays for secreted factors using *InvasiCell*:

Devices with co-cultured invasion assays of MDA MB 231-GFP and MDA MB 231-GFP isolated with fibroblasts were washed 3 times with 1X PBS, and their fixation was performed in 4% paraformaldehyde (PFA) solution in 1X PBS for 15 minutes. After the removal of the round coverslip from the devices, the fixation was continued for 45 minutes. PFA fixation was followed by incubation in a 50 mM glycine solution (pH=7.8) in 1X PBS for 20 minutes. Subsequently, the invasion assays were washed 4 times for 10 minutes in 1X PBS and then blocked with the use of 10% donkey serum (Jackson ImmunoResearch) in 1X PBS for 2 hours. Following that, invasion assays were incubated with primary antibodies in block solution overnight at 4°C. The primary antibodies used in this experiment were: Collagen type III N-terminal rabbit 1:500 (ProteinTech). Then, the primary antibody was washed 4 times with 1X PBS for 10 minutes before the addition of the secondary antibodies in block solution overnight at 4°C. The secondary antibody used in this experiment was: Alexa Fluor® 647 donkey anti-rabbit 1:200 (Jackson Immunoresearch). Afterward, the secondary antibodies were washed 4 times with 1X PBS for 10 minutes. The volume of 500μl of 1XPBS was added to cover the device and then

the device was placed on glass-bottom 35 mm plates (Ibidi). For the imaging, a square cover glass L × W 22 mm × 22 mm, (Sigma Aldrich) was placed on the top of it. Images were obtained by using a Zeiss LSM 910 airyscan laser confocal microscope with the ZEN 2010 software.

7.8 Drug evaluation in cell culture:

All the drug evaluation experiments were conducted using a 50mM stock solution of Doxorubicin hydrochloride (Santa Cruz). MDA MB 231-GFP and MDA MB 231 -GFP isolated were seeded at a density of 50.000 cells per well using a 24-well plate (UltraCruzTM) containing 1 ml DMEM supplemented with 10% FBS. After 24 hours, fresh cell culture media was prepared with the concentrations 87.51μM, 43.76 and 21.87 μM of the drug. Cells were exposed to drug concentration for 24 hours. After that, cell counting was conducted using a hematocytometer for all drug concentrations, and the number of surviving cells was estimated. Then, the obtained values were normalized with the values of untreated cells for each cell line.

7.9 Drug evaluation using *InvasiCell* device:

Invasion assays with MDA MB 231-GFP and MDA MB 231-GFP isolated cells were performed following the previously described protocol. Each device was immersed in 3 ml of DMEM supplemented with 10% FBS containing the concentration of 118 μM. Subsequently, static images were obtained every 24 hours with the same exposure time for each cell line for 3 days by using the Zeiss Axiovert 200M Microscope and Axiovision software (AxioVs40 V 4.7.2.0). The fluorescence intensity indicates the survival of cells was measured and then normalized with the intensities of untreated devices to estimate the cell survival.

7.10 Quantifications and statistical analysis:

All quantifications were performed with the Axiovision LE software, ImageJ, and Zen Blue Edition. Fluorescence intensity was measured using ImageJ. Statistical analysis was performed with the GraphPad Prism software (Prism 8 For Windows, Version 8.01)

RESULTS

8.1 Wound healing assays cannot reliably differentiate cell lines with varying in vivo metastatic potentials

Despite their significant contribution to our understanding of specific events of the metastatic cascade, current in vitro models used in cancer research have several limitations that reduce their in vivo translational potential. These limitations are widely documented in the literature (Katt 2016) and studies have even suggested that evaluating the tumor cells morphology is a more accurate predictor of tumors metastatic potential than using the currently available in vitro assays (Conner, 2024). However, *InvasiCell*, a novel device developed by our group, was shown to accurately replicate the in vivo tumor microenvironment in vitro and allowed the isolation of more metastatic tumor cell populations (Alexandra Manoli, 2022). Therefore, the aim of this study was to examine whether *InvasiCell* can be used as an accurate model to study various aspects of tumor progression, compared to the currently available in vitro tools used in cancer research. Initially, the ability of the existing in vitro models and *InvasiCell* to reflect in vitro the in vivo metastatic potential of tumor cells was evaluated by using already characterized cell lines with known in vivo metastatic potentials. Particularly, three breast cancer cell lines, namely the MCF-7, MDA-MB-231 (MDA), and MDA231-LM2-4175 (LM2) cells which have been classified as non-metastatic, metastatic, and highly metastatic respectively, and two pancreatic cancer cell lines, namely MIA PaCa-2 (PaCa) and Panc-1 (PANC), with PANC been descriped as more metastatic than Paca (Gradiz 2016, Yang 2019, Du 2017), were used for the initial evaluations. Additionally, *InvasiCell* derived cells lines MDA-i and PANC-i, which have been validated in vivo for their increased metastatic potential were compared to their respective parental cell lines by previous in vivo experiments within our lab (Alexandra Manoli, 2022) were also used during these evaluations.

One of the most widely used assays used to evaluate the metastatic potential of tumor cell lines in cancer research is the Wound healing assay, which is a 2D assay that estimates the collective migration abilities of tumor cells by measuring their ability to close a forcefully induce cell free gap. Thus, wound healing assays were performed by using the already characterised breast cancer cell line MCF7, MDA, and LM2, as shown in **Figure 14A**. Interestingly, the collected data showed that the travel distances, estimated by the gap closure over time, between metastatic cell lines such as MDA and LM2 were similar to those of non-metastatic MCF7 cells (**Figure 14B**). Additionally, the metastatic breast cancer cell lines MDA and LM2 exhibited comparable properties in wound healing assays (**Figure 14B**), despite the increased metastatic potential of LM2 compared to MDA in living organisms. In contrast, the MDA-i cells, which displayed increased aggressiveness and metastatic abilities *in vivo*, showed statistically significant higher migration abilities than their parental cell line in Wound healing assays (**Figure 14C and D**).

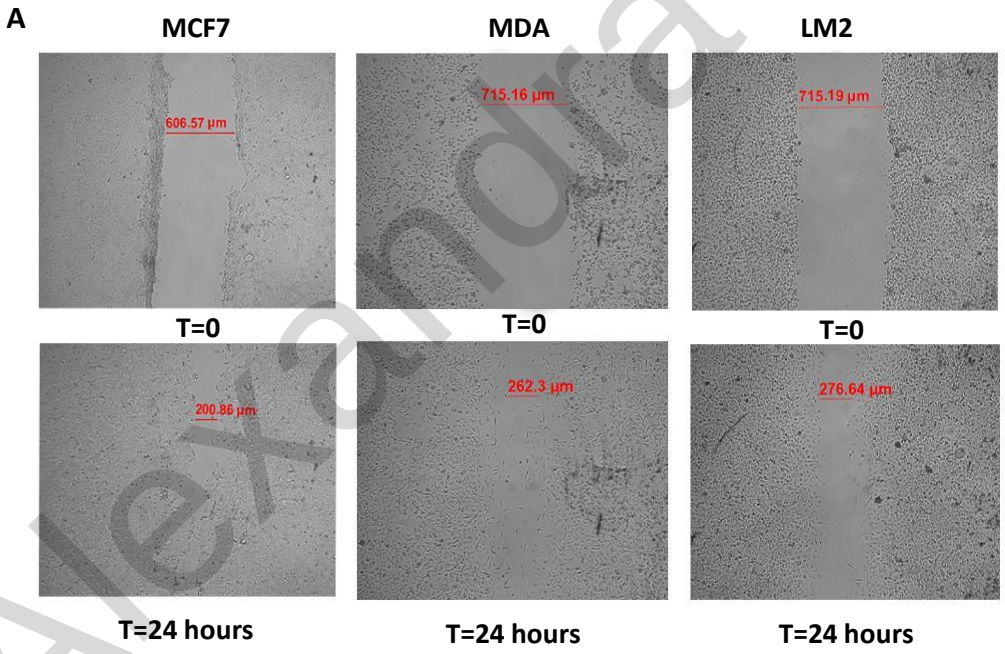

B

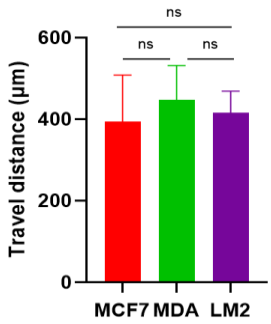

C

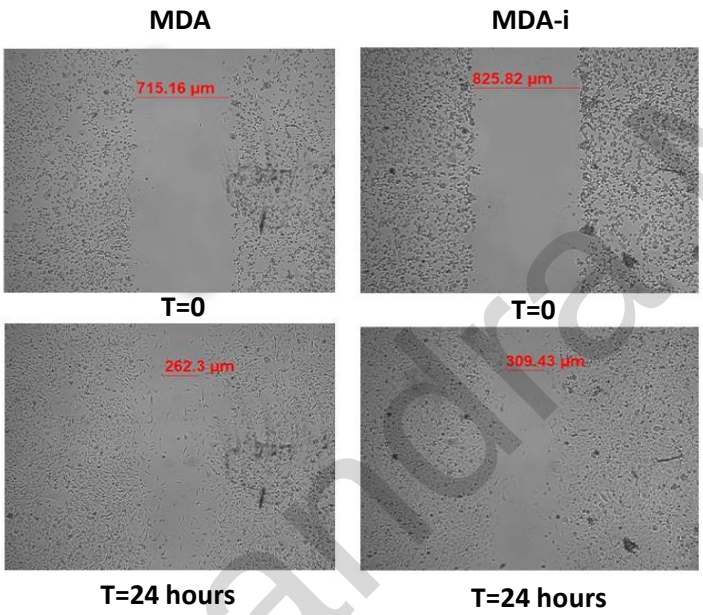

D

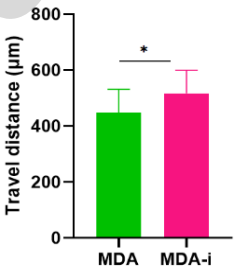

Figure 14: Wound healing assays can weakly distinguish the isolated MDA-i from their parental MDA cells and failed to differentiate other breast cancer cell lines with varying in vivo metastatic potentials. A) Microscope images from live imaging of wound healing assays on t=0 and after 24 hours. The MCF7 cell line is present on the left, the MDA cell line is present on the middle, and the LM2 cell line is present on the right. The gap of MCF-7 wound healing is 606.57 µm at t=0 and 200.86 µm at t=24 hours. The gap of MDA wound healing is 715.16 µm at t=0 and 262.3 µm at t=24 hours. The gap of LM2 wound healing is 715.19 µm at t=0 and 276.64 µm at t=24 hours. **B)** Graphical representation of travel distance for MCF7 (red), MDA (green), and LM2 cells (purple). The travel distance was calculated by the differences between the gap distance at t=0 and the distance gap at =24 hours. **C)** Microscope images from live imaging of wound healing assays on t=0 and after 24 hours. The parental MDA cells are present on the left and the isolated MDA-i cells are present on the right. The gap of MDA wound healing is 715.16 µm at t=0 and 262.3 µm at t=24 hours while the gap of MDA-i wound healing is 825.82 µm at t=0 and 309.43 µm at t=24 hours. **D)** Graphical representation of travel distance for MDA (green), and MDA-i cells (pink). The data were analyzed by one-way ANOVA, Data shown Mean ± S.D. The average was calculated using n= 30 (the measurements of gap-closing for each wound healing at every time point). Bonferroni posttest: P< 0.5 (*), 0.01(**), 0.001 (***).

Similarly, the pancreatic cell lines, PACA and PANC, were used to perform wound healing assays (**Figure 15A**) to evaluate if these cell lines can be differentiated via a Wound healing assay. These evaluations suggest that the PANC cells have significantly higher metastatic potential than PACA cells using wound healing assays (**Figure 15B**). However, comparison of the PANC-i cells with PANC cell line via Wound healing (**Figure 15C**) showed that the *InvasiCell* isolated cells did not display any higher migration abilities than their parental cell line (**Figure 15D**).

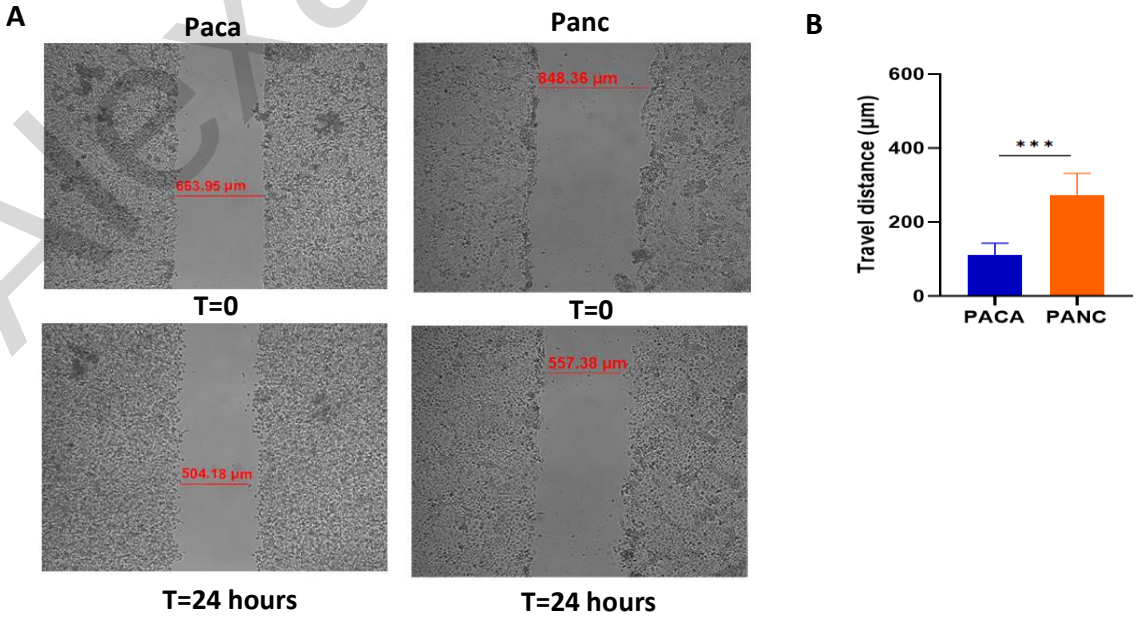

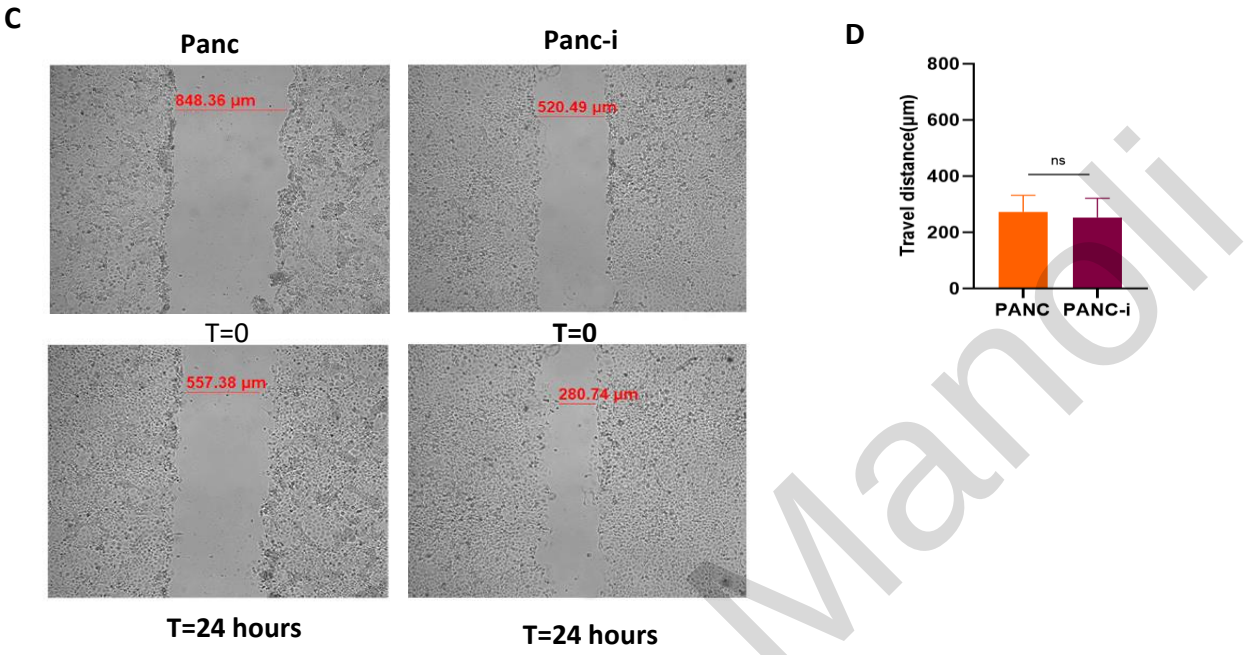

Figure 15: Wound healing assays discriminate between PACA and PANC-1 cells based on their in vivo metastatic capabilities but cannot differentiate the isolated PANC-i and parental PANC cell lines. A) Microscope images from live imaging of wound healing assays on t=0 and after 24 hours. On the left is present the PACA cell line and on the right is the PANC cell line. The gap of PACA wound healing is 663.95 µm at t=0 and 504.18 µm at t=24 hours. The gap of PANC wound healing is 848.36 µm at t=0 and 557.38 µm at t=24 hours. **B)** Graphical representation of travel distance for PACA (blue) and PANC cells (brown). The travel distance was calculated by the differences between the gap distance at t=0 and the distance gap at =24 hours. **C)** Microscope images from live imaging of wound healing assays on t=0 and after 24 hours. On the left is present the PANC cell line and on the right is the isolated PANC-i cell line. The gap of PANC-1 wound healing is 848.36 µm at t=0 and 557.38 µm at t=24 hours µm while the gap of PANC-i wound healing is 520.49 µm at t=0 and 280.74 at t=24 hours. **D)** Graphical representation of travel distance for PANC (brown) and PANC-i cells (dark magenta). The data were analyzed by one-way ANOVA, Data shown Mean ± S.D. The average was calculated using n= 25 (the measurements of gap-closing for each wound healing at every time point). Bonferroni posttest: P< 0.5 (*), 0.01(**), 0.001 (***).

8.2 Boyden chamber assays are unable to distinguish between cell lines with different in vivo metastatic potentials

Considering the inability of wound healing assays to reliably differentiate cell lines with different metastatic abilities *in vivo*, we proceeded to examine our cancer cell lines using Boyden chamber assays. Boyden chamber assay, also known as Transwell migration assay, are the most commonly used 2D in vitro model to evaluate the metastatic potential of tumor cells based on their ability to pass through a porous membrane. In addition, modified Boyden chamber assays have been proposed to enhance the complexity and better mimic the in vivo conditions. Specifically, these assays include an ECM component on the top of chamber insert and evaluate the invasion abilities of cells based on their ability to invade into the ECM barrier and pass through the porous membrane. Initially, Boyden chamber assays were used to evaluate the metastatic potential of the selected cell lines. The collective data about the chosen breast cancer cell lines indicated that the Boyden chamber assays efficiently differentiate the non-metastatic MCF-7 cells from the metastatic MDA and LM2 cells, as both the MDA and the LM2 cell lines showed statistically significant higher percentages of metastatic cells compared the MCF-7 cell line. However, these assays were unable to distinguish between MDA and LM2 cell lines as they showed no statistically significant differences (**Figure 16A)**. Similarly, evaluation of the metastatic potential of the MDA-i cell line, via the Boyden chamber assay, showed no statistically significant differences between the isolated cells and their parental cell line (**Figure 16B)**.

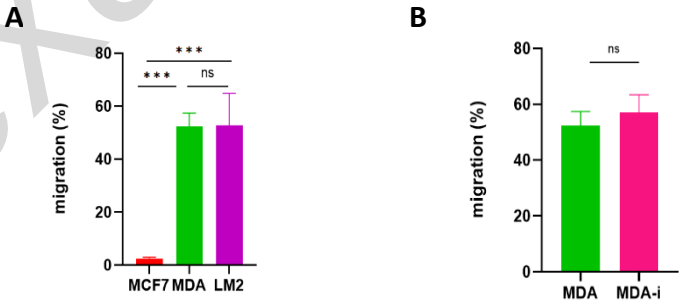

Figure 16: Boyden chamber assays cannot accurately discriminate breast cancer cell lines with different in vivo metastatic potential. The number of 200.000 cells of each cell line was added to the upper chamber of the Boyden chamber insert. After 24 hours, cells that migrated to the lower chamber were trypsinized and counted. The percentage of the migration was calculated by the ratio of migratory cells to the initial cell population. **A)** Graphical representation of the percentage of migration of cells using Boyden chamber assays. The percentage of migration for MCF7 cells is shown in red, for MDA in green, and for LM2 in purple. **B)** Graphical representation of the percentage of migration for the parental MDA (green) and isolated MDA-i cells (pink) using Boyden chamber assays. The data was analyzed by one-way ANOVA, Data represents Mean ± S.D. The data was calculated using n=3 chambers (for each cell line) Bonferroni posttest: P< 0.5 (*), 0.01(**), 0.001 (***).

Moreover, similar observation was made when the Boyden chamber assays were used to evaluate the metastatic potential of the pancreatic cancer cell lines. Specifically, the collected data illustrated that there are no statistically significant differences between the metastatic potentials of the PANC from PACA cell lines (**Figure 17A)** or the isolated PANC-i cell line from their parental cells **(Figure 17B).** This is quite surprising given the fact that a wound healing assay could better capture the differences in metastatic potential between PANC and PACA than the Boyden chamber-based assay and demonstrates that these assays only capture a small fraction of the conditions inside a tumor and thus the characteristics that a cell must exhibit to display increased invasion are very narrow and fail to accurately represent the *in vivo* invasive capacity of the cell.

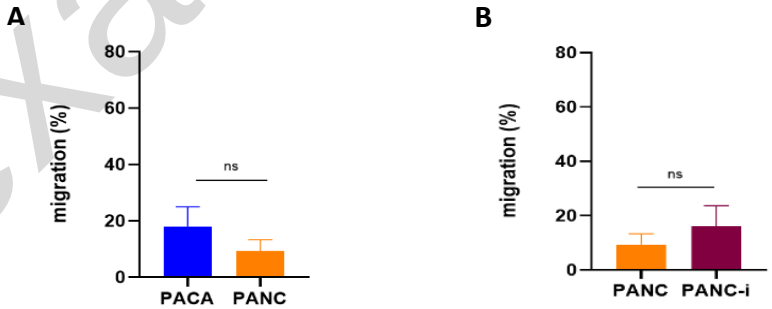

Figure 17: Boyden chamber assays cannot differentiate any of the pancreatic cell lines with varying in vivo metastatic potentials. A) Graphical representation of the percentage of migration of cells using Boyden chamber assays. The percentage of migration for PACA cells is shown in blue and for PANC cells is shown in orange. **B)** Graphical representation of the percentage of migration for the parental PANC (orange) and isolated PANC-i cells (dark magenta) using Boyden chamber assays. The data was analyzed by one-way ANOVA, Data represents Mean ± S.D. The data was calculated using n=3 chambers (for each cell line) Bonferroni posttest: P< 0.5 (*), 0.01(**), 0.001 (***).

Given that Boyden chambers were ineffective to reflect the *in vivo* metastatic potential of the tested cell lines, modified Boyden chamber assays were performed by coating the Boyden chamber inserts with collagen. Particularly, we wanted to assess whether this approach could increase the accuracy of these assays to distinguish tumor cells with validated *in vivo* different metastatic capabilities. During this experiment, both isolated cell lines were used and compared to the respected parental cell lines, as none of these cell lines showed significant differentiation in Boyden chamber assays. These evaluations showed that neither of the isolated MDA-i and Panc-i cell populations have altered metastatic potential than their respected parental cell lines (**Figure 18A and 18B**), despite the elevated metastatic abilities of isolated cell lines observed *in vivo*.

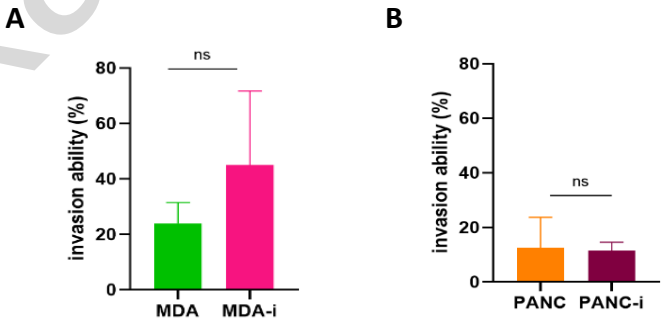

Figure 18: Modified Boyden chamber assays were unable to distinguish the isolated from their parental cell populations. The number of 500.000 cells was added to the upper chamber coated with 0.125% collagen gel of the insert. After 24 hours, the cells that invaded to the lower chamber were trypsinized and counted. The percentage of the invasion was calculated by the ratio of invaded cells to the initial cell population. **A)** Graphical representation of the percentage of invasion for the parental MDA (green) and the isolated MDA-i cells (pink) using modified Boyden chamber assays. **B)** Graphical representation of the percentage of invasion for the parental PANC cells (orange) and the isolated PANC-i cells (dark magenta) using the modified Boyden chamber assays. The data was analyzed by one-way ANOVA, Data represents Mean ± S.D. The data was calculated using n=3 chambers (for each cell line) Bonferroni posttest: P< 0.5 (*), 0.01(**), 0.001 (***).

8.3 Tumor spheroids-based methods display an improved predictive ability of the in vivo metastatic potential compared to other assays but are plagued by various challenges making them challenging to implement

Tumor spheroid-based assays are considered the gold standard 3D *in vitro* tool used in cancer research, thus we attempted to generate tumor spheroids for our breast and pancreatic cell lines. The first challenge we faced was the lack of a standardized protocol for generating tumor spheroids. As described in the introduction, there are several techniques used to generate 3D culture spheroids, such as the non-scaffold system where cells are in suspension or the scaffold-based system where cells are embedded into a collagen gel. Studies demonstrated that the choice of method for generating spheroids can vary depending on the ability of the examined cell line to form spheroids, even when using the same type of cancer cell lines (Stadler 2018, Gheytanchi, 2021). The capacity of cells to generate spheroids has been associated with the expression level of cadherins that is essential to form adherent junctions (Stadler 2018). Therefore, we performed several to optimize the protocol which resulted in the effective generation tumor spheroids using our breast and pancreatic cell lines (**Figure 19**). Initially, we tested a scaffold-based system using hydrogel to create tumor spheroids. Specifically, we made our plates low adherent by using 1% agarose gel and then we embedded a small number of tumor cells in a hydrogel. We found that

generating spheroids using this technique is time-consuming because the formation of spheroids can begin from even a single cell. The aggregates of MDA cells 15 days after the embedding into collagen gel are shown in **Figure 19A**. We observed that the cell clusters remained small in size after 15 days of embedding, resulting in cell death, and failed to migrate into the collagen gel. In an effort to overcome this, we used a non-scaffold system, the hanging drop technique to generate spheroids and subsequently the cell aggregates were embedded in a collagen gel using low-adherent plates. Although tumor cells generated aggregates in a few days, when we embedded the spheroids in gels, they were dissociated and became small cell clusters. Additionally, we observed within the next two days after the embedding, tumor spheroids fully disassociated because cells were loosely attached within aggregates (**Figure 19B**). Considering the above observation, we included Matrigel within the hanging droplet to support the tight cell-to-cell interactions. However, the spheroids were destroyed while embedding them in collagen gel, and in the following days cell aggregates disassociated (**Figure 19C**).

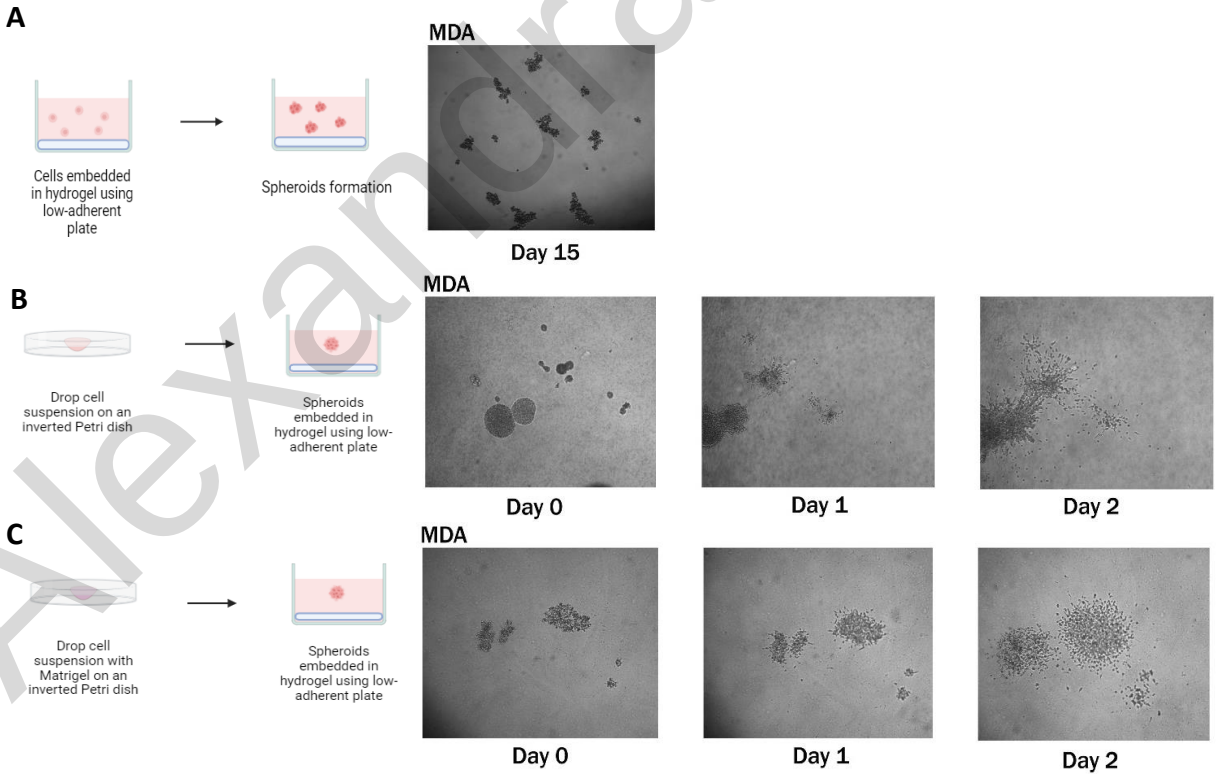

Figure 19: Unsuccessful techniques for generating MDA tumor spheroids. A) Scaffolding-based model. The cells were embedded in the hydrogel using a low-adherent plate. The cells are allowed to form spheroids. On the right, microscope images of MDA cells aggregates taken 15 days post-embedding. **B)** Hanging drop method. A drop of cell suspension in media is placed on the lid of the Petri dish which is then placed inverted over the Petri dish. The Petri dish contains PBS to generate humidity and cells are allowed to generate spheroids for 5-7 days. Following, the tumor spheroids are embedded in collagen gel. Microscope images of MDA cells aggregates are shown on Day 0 (day of embedding), Day 1, and Day 2 post-embedding. **C)** Hanging drop method using an ECM component in the drop of cells. A droplet of cell suspension in media containing Matrigel is placed on the lid of the Petri dish. Then, the lid is placed inverted over the Petri dish, and cells are allowed to generate spheroids for 5-7 days. After that, the tumor spheroids are embedded in a collagen gel. Microscope images of MDA cells aggregates are present on Day 0 (day of embedding), Day 1, and Day 2 after embedding.

After optimizing the protocol to generate tumor spheroids (described in Material and Method section), we successfully generated tumor spheroids for all breast and pancreatic tumor cells, which were used to evaluate and compare the metastatic potential of the different cell lines. Evaluation of the breast cancer cell lines showed that MCF7 can be differentiated as their spheroids showed significantly lower invasive potential than those from the metastatic MDA and highly metastatic LM2 tumor cell lines. However, LM2 tumor spheroids did not reflect the elevated *in vivo* metastatic potential of LM2 compared to MDA cells (**Figure 20A**). Interestingly, according to tumor spheroids results, MDA cells were shown to be significantly more metastatic compared to LM2 which is in contrast with their metastatic potential observed *in vivo* (**Figure 20B**). Following this, we continued to examine if the isolated MDA-i cell which showed statistically significant higher metastatic potential than their parental MDA cells *in vivo* using tumor spheroids (**Figure 20C)**. The collected data suggested that the tumor spheroids technique can distinguish the isolated MDA-i cells from their parental MDA cells within 24 hours (**Figure 20D**).

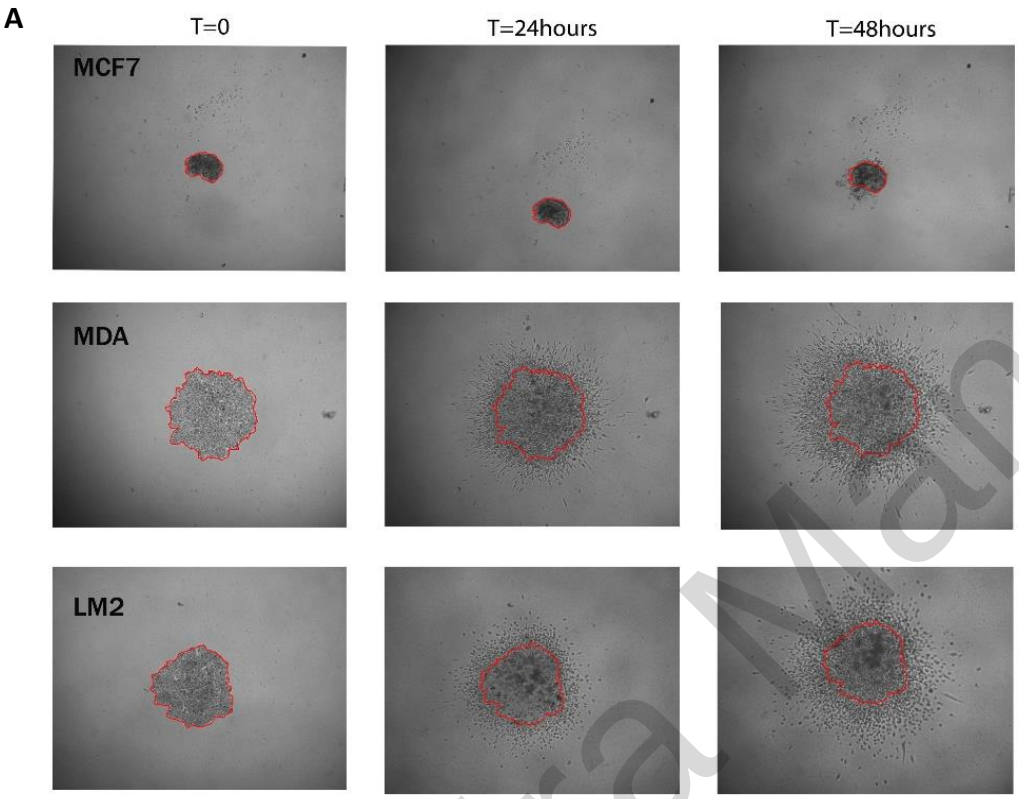

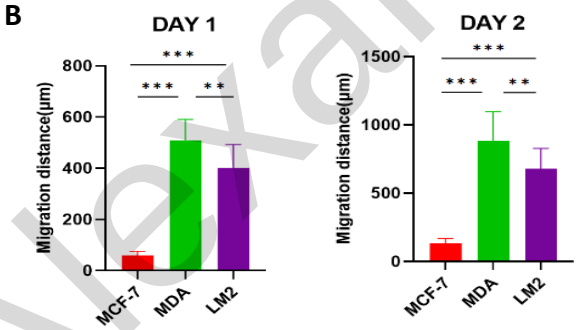

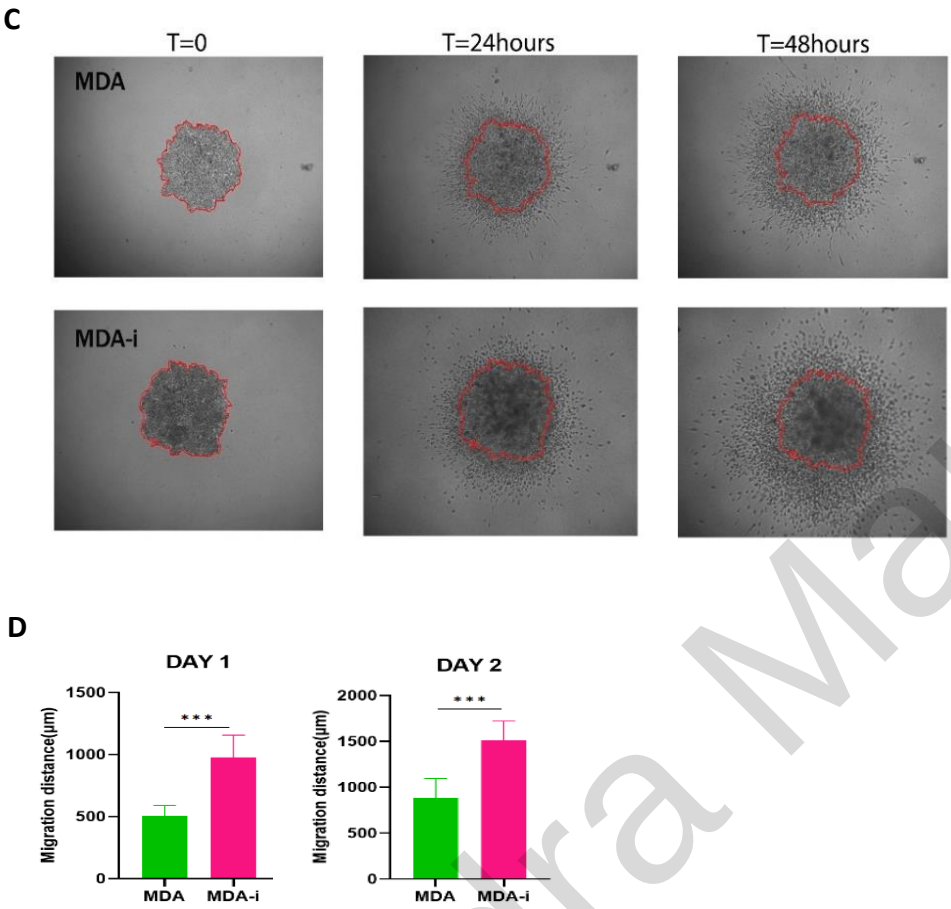

Figure 20: Tumor spheroid assays can differentiate the breast cancer cell lines with varying in vivo metastatic abilities apart from the LM2 cell line. Breast cancer cell lines were used to generate tumor spheroids. The number of 2500 cells per well were cultured in a low adherent 96-plate and were allowed to form spheroids for 48 hours. After that, the spheroids were embedded in collagen gels and static images were obtained over time. **A)** Images of tumor spheroids for MCF7, MDA and LM2 cell lines at T=0, T=24 hours and T= 48 hours. The red outlines show the initial tumor spheroid size at T=0. **B)** Graphical representation of migration distances (µm) for MCF7 (red), MDA (green) and LM2 (purple) cells from the initial spheroid area at 24 hours (Day1) and 48 hours (Day2). **C)** Images of tumor spheroids for the parental MDA cells and isolated MDA-i cells at T=0, T=24 hours and T= 48 hours. **D)** Graphical representation of the migration distance for MDA (green) and MDA-i (pink) cells from the initial spheroid area 24 hours (Day1) and 48 hours (Day2). The data was analyzed by one-way ANOVA, Data represents Mean ± S.D. The data was obtained by measurements of distance from leader cells to the initial spheroid area using n=6 spheroids (for each cell line) Bonferroni posttest: P< 0.5 (*), 0.01(**), 0.001 (***). All brightfield images were obtained using 5X objective.

Similarly to the breast cancer cell lines, tumor spheroids for the PACA and PANC cells were generated to investigate if the tumor spheroids of pancreatic tumor cells replicate their differences in metastatic potentials *in vivo* (**Figure 21A**). Our data showed that the tumor spheroid assay significantly distinguished between the more aggressive PANC cells and PACA cells within 24 hours (**Figure 21B**). In addition, we proceeded to study if the isolated PANC-i and the parental PANC cells can be differentiated for their different metastatic abilities using the tumor spheroid method (**Figure 21C**). Collected data from the tumor spheroids technique showed that this assay effectively differentiated the isolated PANC-i cells which displayed increased metastatic abilities *in vivo* compared to their parental PANC cells (**Figure 21D)**.

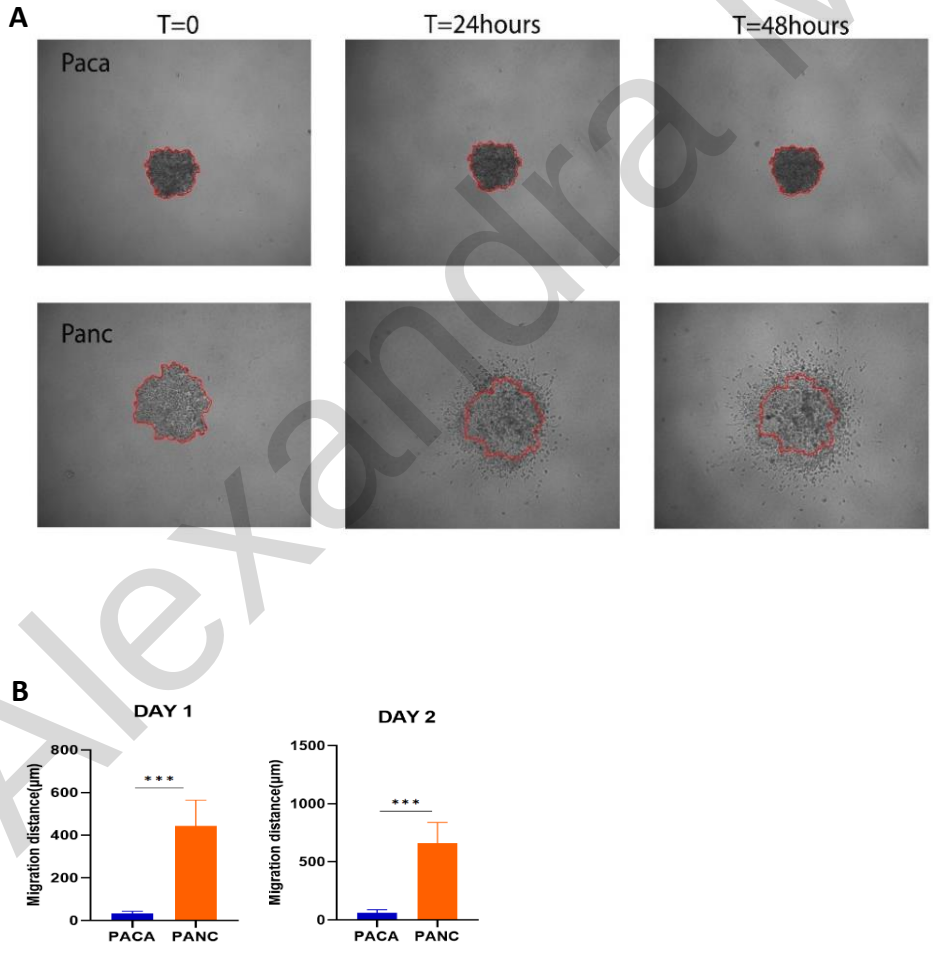

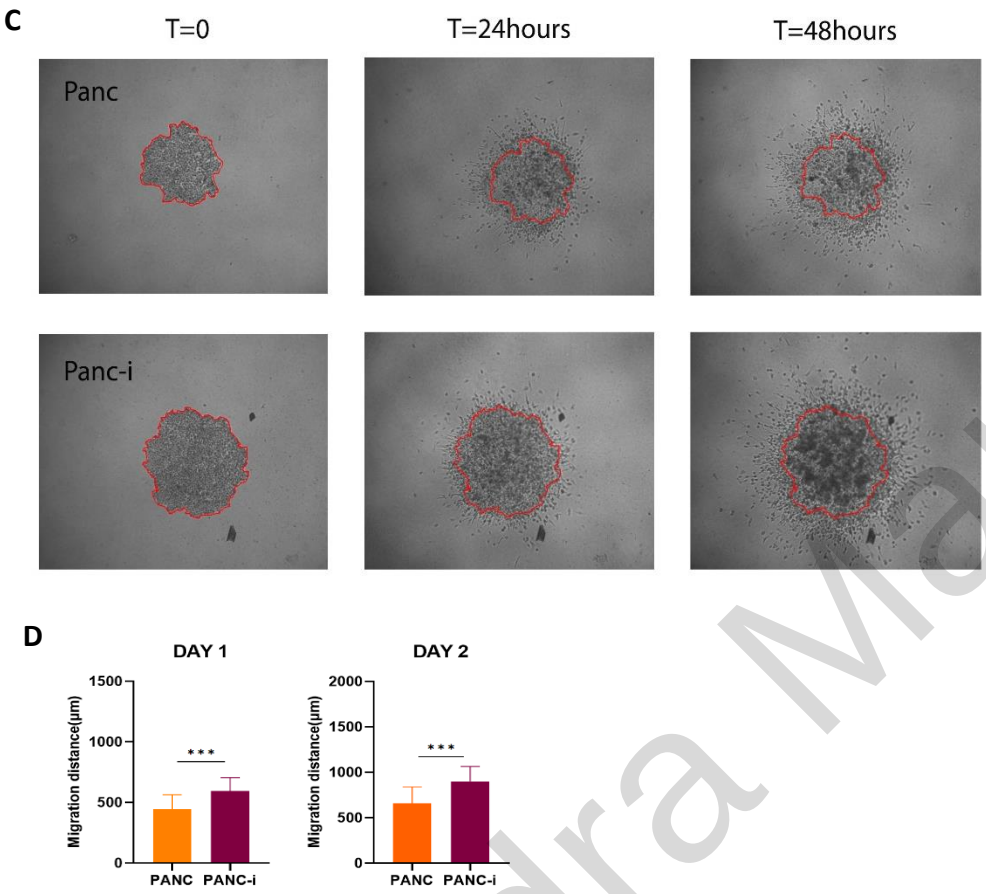

Figure 21: Tumor spheroid assays can discriminate all the pancreatic cell lines with varying in vivo metastatic abilities. Pancreatic cancer cell lines were used to generate tumor spheroids. The number of 2500 cells per well were cultured in a low adherent 96-plate and were allowed to form spheroids for 48 hours. After that, the spheroids were embedded in collagen gels and static images were obtained over time. **A)** Images of tumor spheroids for PACA and PANC cell lines at T=0, T=24 hours and T= 48 hours. The red outlines show the initial tumor spheroid size at T=0. **B)** Graphical representation of migration distances (µm) for PACA (blue) and PANC (orange) cells from the initial spheroid area at 24 hours (Day1) and 48 hours (Day2). **C)** Images of tumor spheroids for the parental PANC cells and isolated PANC-i cells at T=0, T=24 hours and T= 48 hours. **D)** Graphical representation of the migration distance for PANC (orange) and PANC-i (dark magenta) cells from the initial spheroid area 24 hours (Day1) and 48 hours (Day2). The data was analyzed by one-way ANOVA, Data represents Mean ± S.D. The data was obtained by measurements of distance from leader cells to the initial spheroid area using n=6 spheroids (for each cell line) Bonferroni posttest: P< 0.5 (*), 0.01(**), 0.001 (***). All bright-field images were obtained using 5X objective.

8.4 *InvasiCell* reflects the *in vivo* metastatic potential of cancer cell lines more accurately and reliably compared to other assays including spheroid assays

Following the evaluation of the metastatic potentials of the selected cell lines with the most commonly used techniques and methods that are used in cancer research, we proceeded to examine whether *InvasiCell* could differentiate more reliably cell lines with varying *in vivo* metastatic potentials than other in vitro tools. Initially, we performed invasion assays to study the invasive potentials of breast cancer MCF7, MDA, and LM2 cell lines which had been characterized for their different in vivo metastatic potentials. The collected data suggests that the *InvasiCell* distinguishes the cell lines based on their in vivo metastatic potentials, as the highly metastatic LM2 cells showed statistically significant higher metastatic potential than both the MDA and MCF-7 cell lines (**Figure 22A and B**). Specifically, LM2 cells invaded the entire invasion zone 16 days after the setup of invasion assays, while MDA cells had 268.28 μm until the edge of the invasion zone. Furthermore, the non-metastatic MCF7 cells barely moved outside the core of the device by day 16 as they traversed only 417.72 μm from the core (**Figure 22A**). Therefore, *InvasiCell* was able to differentiate between these breast cancer cell lines with different in vivo metastatic potentials on day 16 (**Figure 22B**). Also, the LM2 cells were able to exit the invasion zones of *InvasiCell* one day earlier than the metastatic MDA cells. Additionally, we observed that the invasion rate of MCF7 cells within the *InvasiCell* replicates their non-metastatic abilities from the first days of invasion assays compared to the metastatic MDA and LM2 cells (**Figure 22C**).

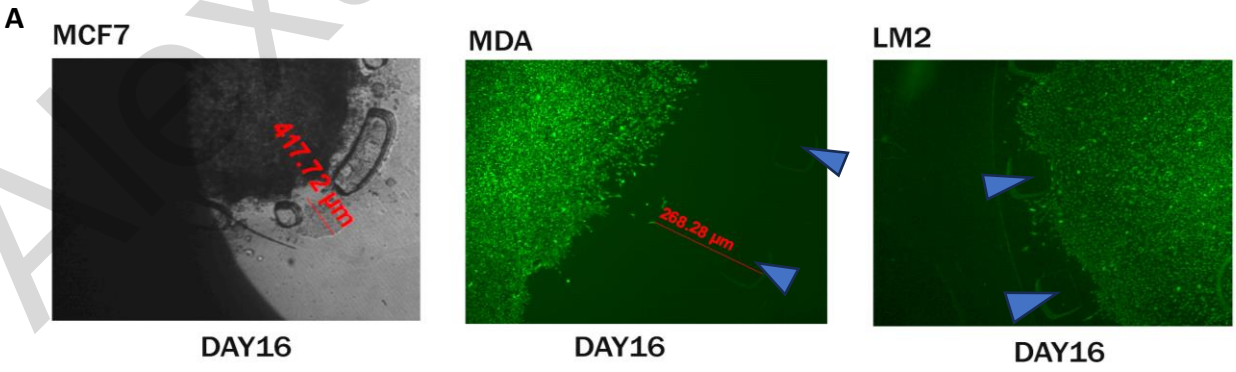

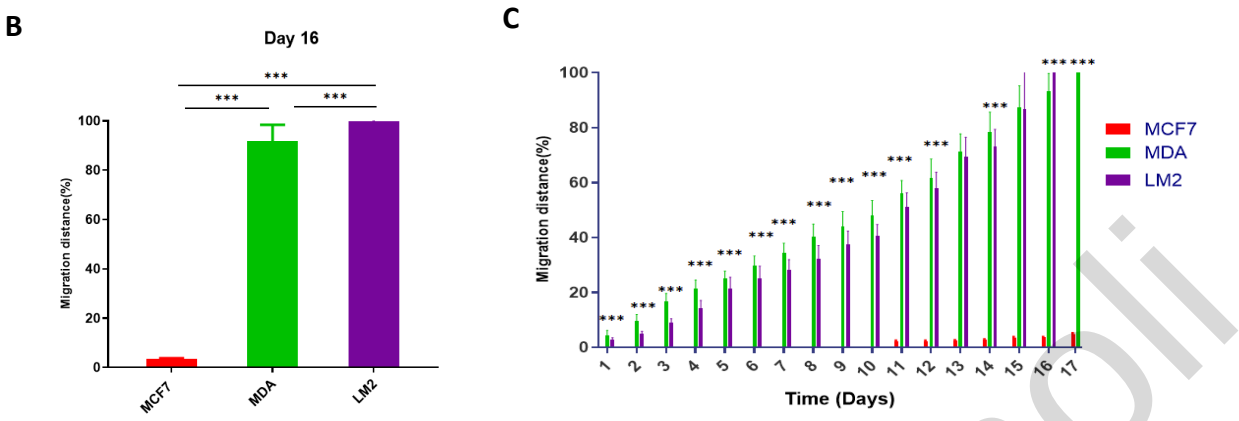

Figure 22: *InvasiCell* effectively distinguishes between breast cancer cell lines with varying in vivo metastatic potentials. A) Microscope images of MCF7 (left), MDA (middle), and LM2 (right) cell lines 16 days post introduction in *InvasiCell*. MCF7 managed to invade only 417.72 µm distance from the core of the device in 16 days. LM2 cells reach the end of the invasion zone (blue arrows) in 16 days compared to MDA cells which are 268.68 µm from the end of the invasion zone. **B)** Graphical representation of the percentage of migration within *InvasiCell* of MCF7 (red), MDA (green), and LM2 (purple) on day 16. **C)** Graphical representation of the percentage of migration within *InvasiCell* of MCF7 (red), MDA (green), and LM2 (purple) over a period of 17 days. The data were analyzed by two-way ANOVA, Data shown Mean ± S.D. The average was calculated using n=30 (the number of measurements taken each day for each cell line. Bonferroni posttest : P< 0.5 (*), 0.01(**), 0.001 (***).

Subsequently, we conducted invasion assays to assess whether *InvasiCell* could reflect the parental MDA and isolated MDA-i cell population *in vivo* metastatic potential. The analysis showed that the isolated MDA-i cells have higher metastatic potential within *InvasiCell* as they traversed and exited the invasion zone after 15 days, whereas MDA cells were 389.97 µm away from the end of the invasion zone (**Figure 23A**). Interestingly, the isolated MDA-i cells showed significant and sustained increased metastatic potential from their parental MDA cells starting from day 5 and remaining until the day they exit (**Figure 23B and C**).

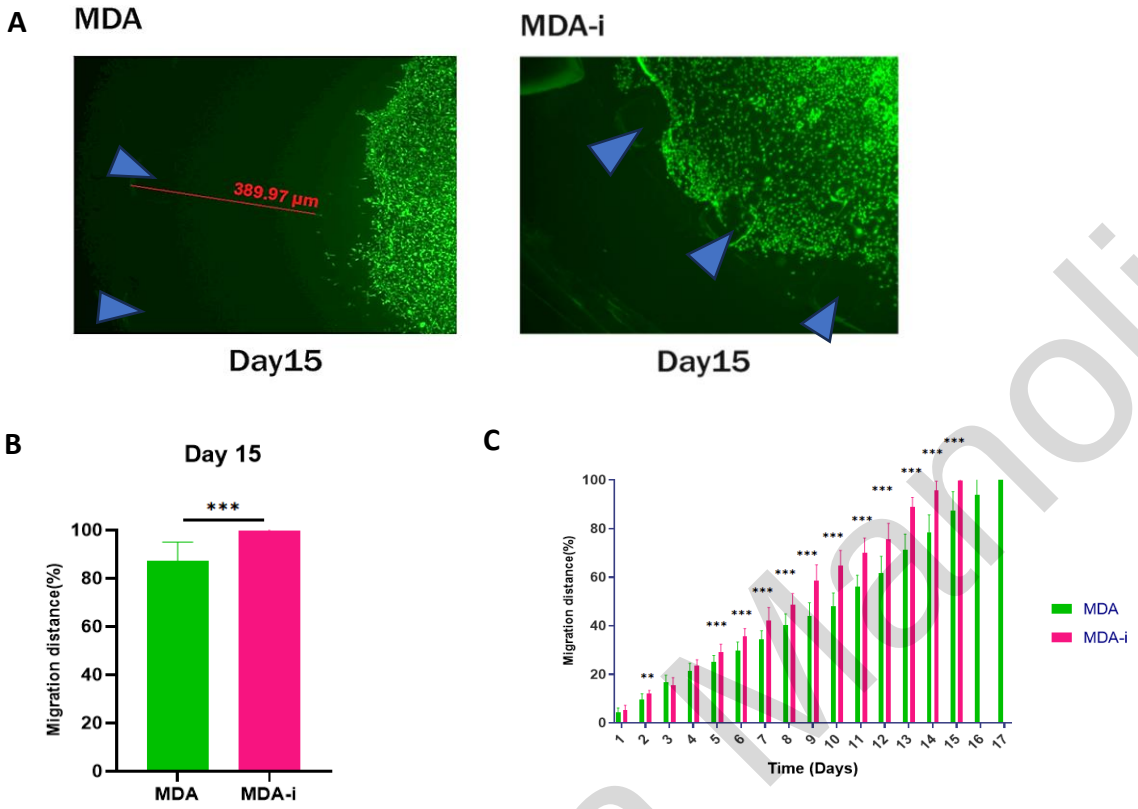

Figure 23: *InvasiCell* successfully discriminates the isolated MDA-i cells which displayed increased in vivo metastatic potential from their parental MDA cells. A) Microscope images of MDA (left) and MDA-i (right) cell lines 15 days post introduction in *InvasiCell*. Isolated MDA-i cells invade and reach the end of the invasion zone (blue arrows) in 15 days compared to parental MDA cells which are 389.97 µm from the end of the invasion zone. **B)** Graphical representation of the percentage of migration within *InvasiCell* of MDA (green) and MDA-i (pink) on day 15. **C)** Graphical representation of the percentage of migration within *InvasiCell* MDA (green) and MDA-i (pink) over a period of 17 days. The data were analyzed by two-way ANOVA, Data shown Mean ± S.D. The average was calculated using n=30 (the number of measurements taken each day for each cell line. Bonferroni posttest : P< 0.5 (*), 0.01(**), 0.001 (***).

Considering that all the breast cancer cell lines with different *in vivo* metastatic potentials were distinguished using *InvasiCell*, we moved on to examine whether the pancreatic cancer cell lines could also be differentiated by *InvasiCell*. Similarly, the PACA and PANC cell lines were used to set-up *InvasiCell* devices. Collectively our data illustrated that the PANC cells traversed and exited from the invasion zone faster than the PACA cells. As shown in **Figure 24A**, PANC cells required 41 days to invade and exit the invasion zone, while PACA cells had a 2243.72 µm distance until the edge of the invasion zone. Thus, PACA cells exhibited a significantly reduced invasion compared to PANC cells (**Figure 24B**). Additionally, we observed that the PANC cells showed significantly increased invasion rates compared to the PACA cells in the first three days (**Figure 24C**) despite the long period PANC cell line required to exit the device.

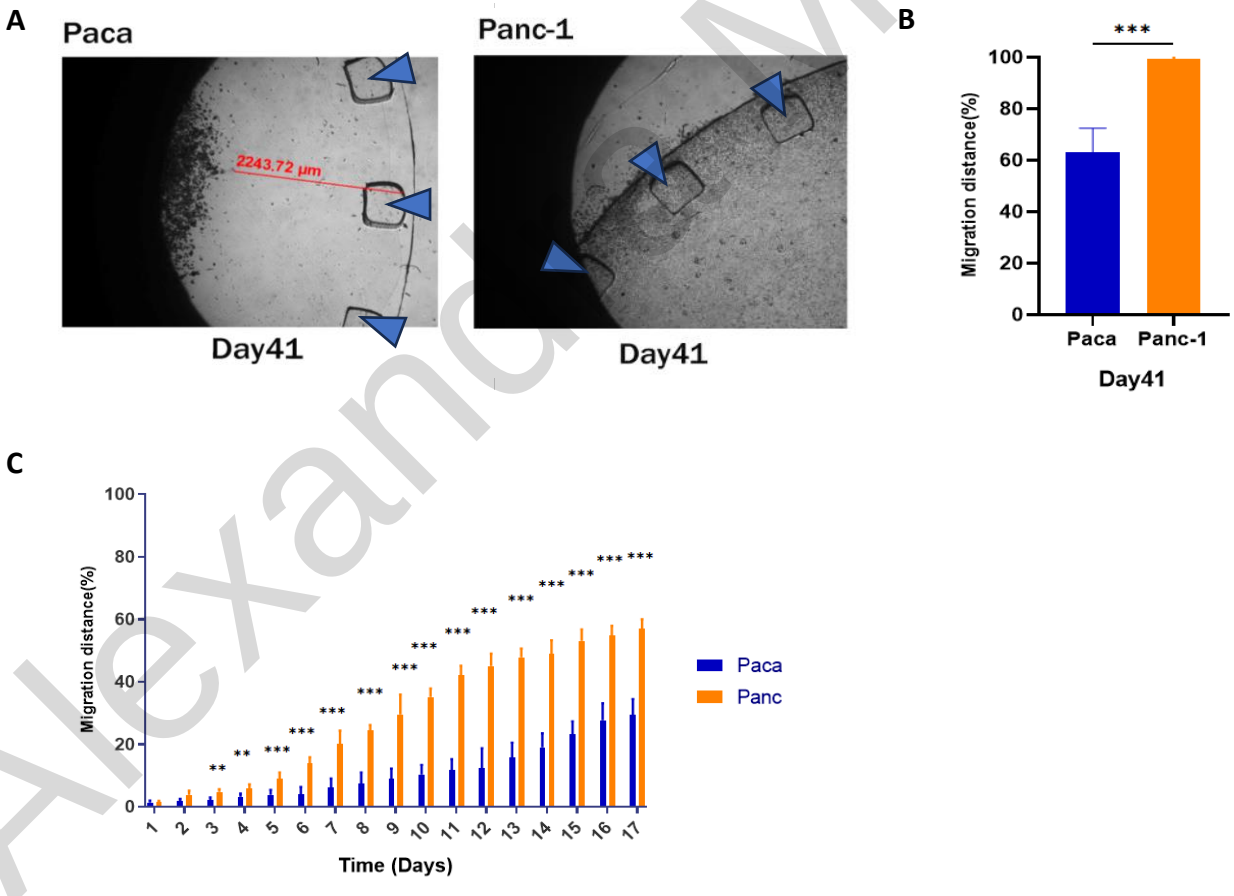

Figure 24: *InvasiCell* effectively differentiates between Paca and Panc cells in few days. A) Microscope images of PACA (left) and PANC (right) cell lines 41 days post introduction in *InvasiCell*. PANC cells invade and reach the end of the invasion zone (blue arrows) in 41 days compared to PACA cells which are 2243.72 μm from the end of the invasion zone. **B)** Graphical representation of the percentage of migration within *InvasiCell* of PACA (blue) and PANC (orange) on day 41. **C)** Graphical representation of the percentage of migration within *InvasiCell* PACA (blue) and PANC (orange) over a period of 17 days. The data were analyzed by two-way ANOVA, Data shown Mean ± S.D. The average was calculated using n=30 (the number of measurements taken each day for each cell line. Bonferroni posttest : P< 0.5 (*), 0.01(**), 0.001 (***).

Findings from our lab validated that the isolated PANC-i cells displayed higher metastatic potential *in vivo* compared to their parental PANC cells. According to previously data, only the tumor spheroids technique was able to discriminate these cell populations. Thus, we conducted invasion assays to study whether this differentiation could be achieved by using *InvasiCell*. The analysis revealed that isolated PANC-i cells exited from the device eleven days earlier than their parental PANC cells. Specifically, by day 30 when the isolated PANC-i cells exited the invasion zone of the device, the parental PANC cells had to invade 2496.62 μm until the edge of the invasion zone (**Figure 25A**). Therefore, the PANC-i cells displayed a significantly increased metastatic potential than their parental cell within *InvasiCell* (**Figure 25B**). This data indicates that *InvasiCell* can replicate the difference between the in vivo metastatic abilities of these cell populations.

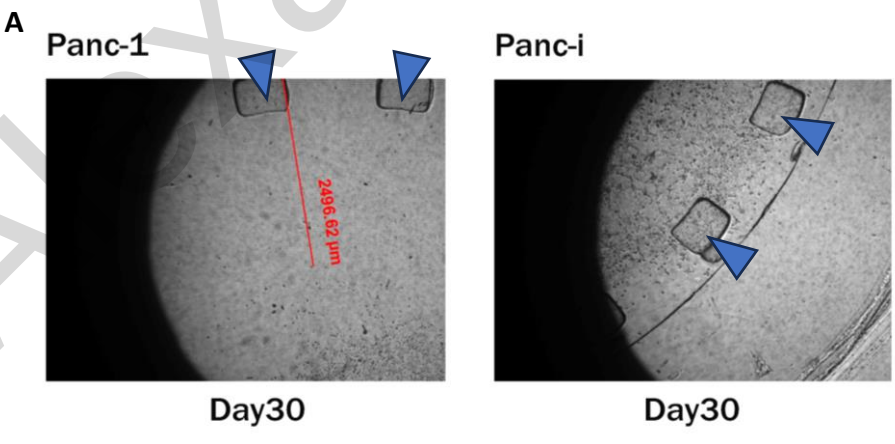

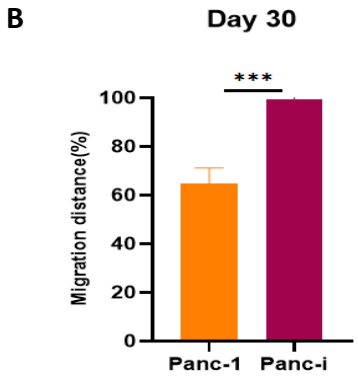

Figure 25: *InvasiCell* replicates the difference between the in vivo metastatic potentials of parental PANC and isolated PANC-i cells. A) Microscope images of PANC (left) and PANC-i (right) cell lines 30 days post introduction in *InvasiCell*. The PANC-i cells invade and reach the end of the invasion zone (blue arrows) in 30 days compared to parental PANC cells which are 2496.62 μm from the end of the invasion zone. **B)** Graphical representation of the percentage of migration within *InvasiCell* of PANC (orange) and PANC-i (dark magenta) on day 30. The data were analyzed by two-way ANOVA, Data shown Mean ± S.D. The average was calculated using n=30 (the number of measurements taken each day for each cell line. Bonferroni posttest : P< 0.5 (*), 0.01(**), 0.001 (***).

8.5 The inclusion of NIH/3T3 fibroblasts within *InvsiCells* core reduces the invasion rates of breast tumor cells

The tumor microenvironment consists of various cell types besides the tumor cells as stromal cells and immune cells, with fibroblasts been the most abundant stromal cells present in the surrounding tissue of a tumor. Several studies demonstrate their controversial role in cancer progression acting both as tumor-promoting or tumor-suppressive (Feng, 2022). Thus, we wanted to investigate whether the presence of NIH3T3 fibroblasts within the *InvasiCell* could affect the invasive capacity of cells. Furthermore, we also aimed to examine if the fibroblasts could improve the ability of *InvasiCell* to reflect the *in vivo* metastatic potential of tumor cells. Therefore, *InvasiCell* devices were set-up by introducing fibroblast within the tumor cell core sample at a ratio of 1:5. Our data showed that a small number of fibroblasts managed to survive

and exit the core of the device over time (**Figure 26A**). In addition, quantification of the invasion potential of cell showed that all examined cell lines displayed a delay in their invasion abilities compared to their invasion rates within *InvasiCell* without fibroblasts. As shown in **Figure 26B**, when fibroblasts were included with MDA cells, the reduction in their invasion rate became significant compared to the MDA invasion rate after 13 days. However, isolated MDA-i and LM2 with the presence of fibroblasts displayed a remarkable reduction in their invasion abilities on 5 days and maintained compared to their invasion potentials without fibroblasts. Specifically, MDA cells with fibroblasts invaded and covered the entire invasion zone in 21 days. Despite the increased in vivo metastatic potentials of MDA-i and LM2 cells compared to MDA cells, cells exited the invasion zone on days 22 and 23 respectively when we included fibroblasts (**Figure 26C**).

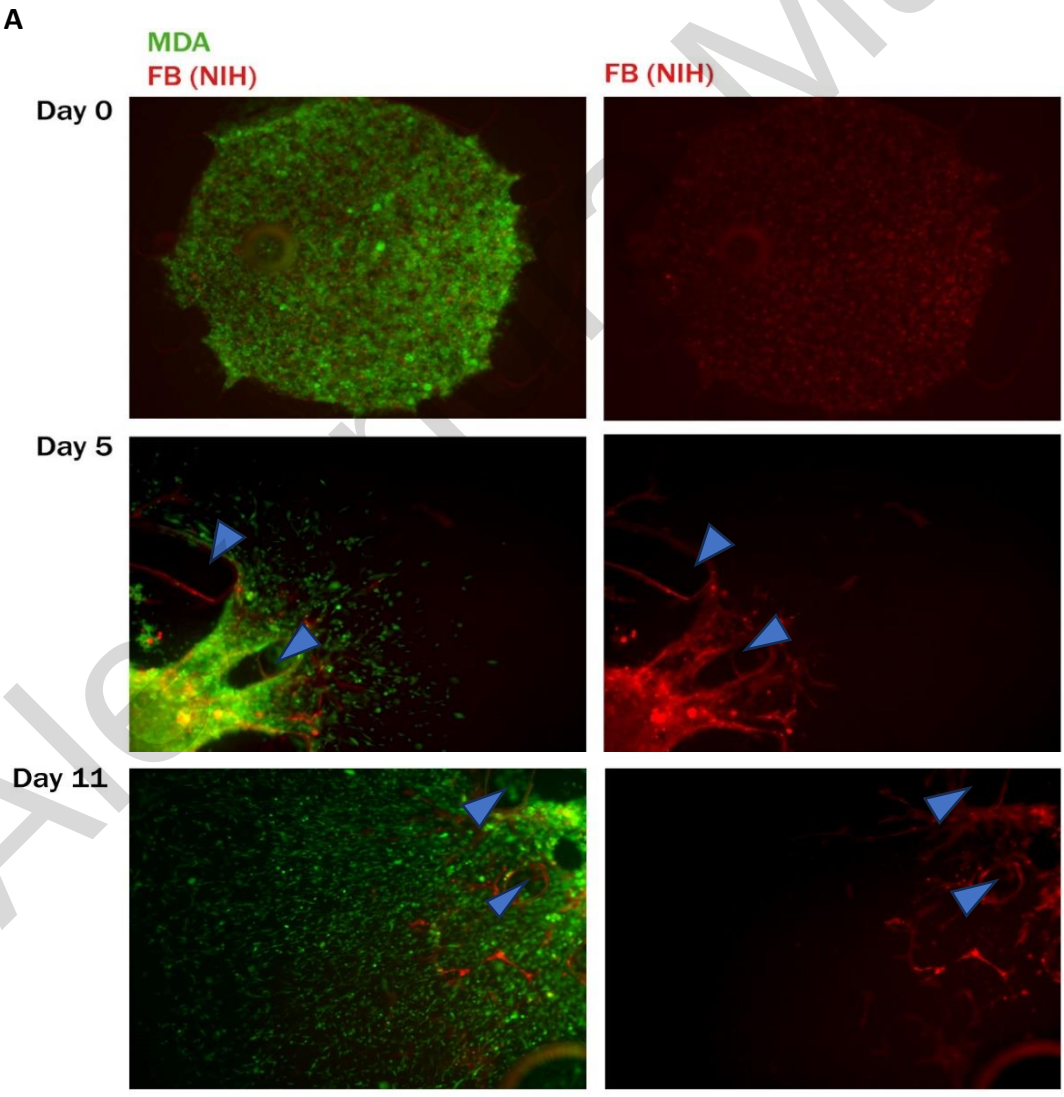

B

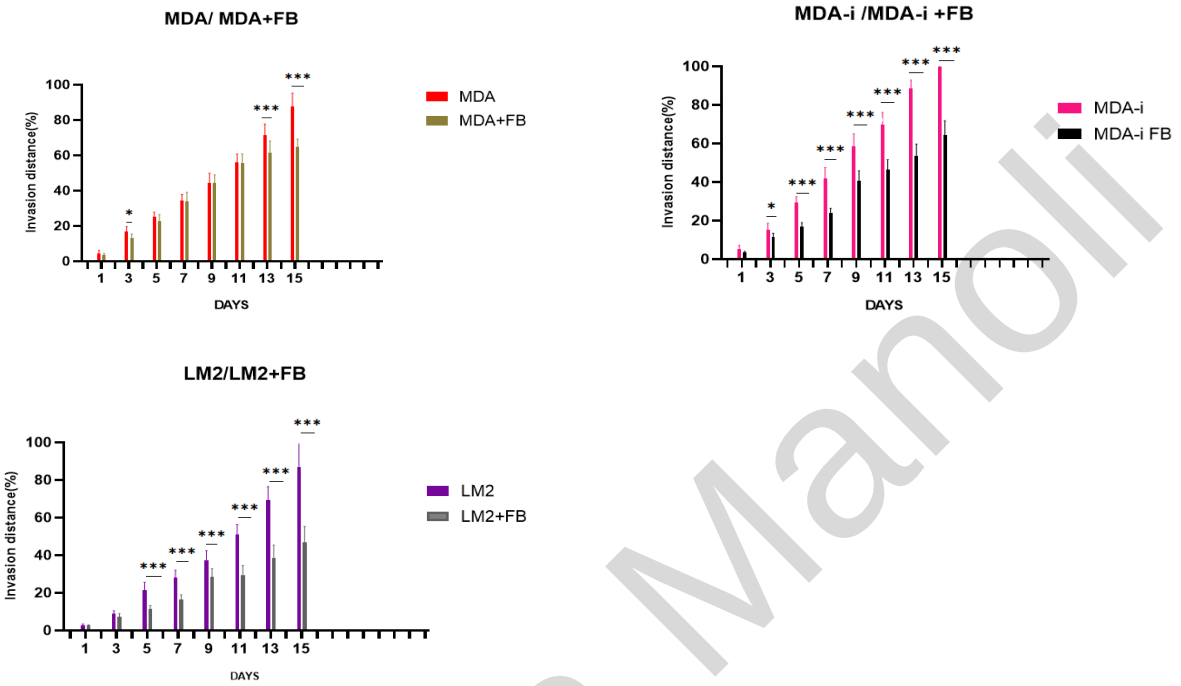

C

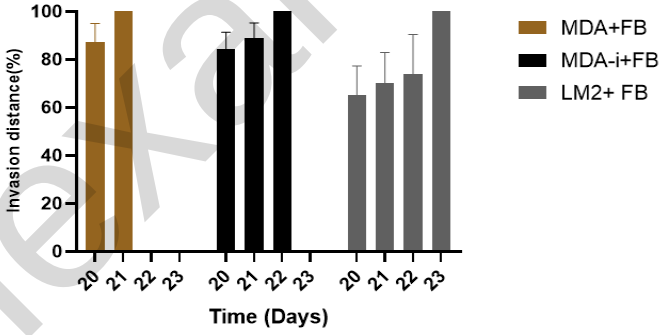

Figure 26: The presence of fibroblasts reduces the invasion abilities of the tumor cells and leads to a reduction of the assay to differentiate cells based on their in vivo metastatic potential. A) Fluorescent images of MDA invasion assays including fibroblasts in the core of the device at days 0, 5, and 11. MDA cells are shown in green and NIH fibroblasts are shown in red. The blue arrows demonstrate the boundaries of the core of InvasiCell. **B)** Graphical representation of the percentage of invasion for MDA (red)/MDA with fibroblasts (brown), MDA-i (pink)/MDA-i with fibroblasts (black), and LM2 (purple)/ LM2 with fibroblasts (grey) using *InvasiCell*. **C)** Graphical representation of the percentage of invasion using MDA with fibroblasts (brown), MDA-i with fibroblasts (black), and LM2 with fibroblasts (grey). This graph demonstrates the exact day when cells exit the invasion zone of the device. Specifically, MDA cells with fibroblasts (brown) required 21 days to invade and reach the edge of the invasion zone, while MDA-i with fibroblasts (black) and LM2 with fibroblasts (grey) needed 22 and 23 days respectively. The data were analyzed by two-way ANOVA, Data shown Mean ± S.D. The average was calculated using n=20 (the number of measurements taken each day for each cell line. Bonferroni posttest : P< 0.5 (*), 0.01(**), 0.001 (***).

As mentioned in the introduction, fibroblasts are responsible for the ECM remodeling within the tumor microenvironment. Additionally, previous data suggested that the presence of fibroblasts in the core of the device along with tumor cells leads to a delay in the invasive potentials of tumor cells. Therefore, we wanted to examine whether the presence of fibroblasts alters the deposition of ECM components. We proceeded by performing Immunofluorescence staining for collagen type III on invasion assays of MDA-i cells with fibroblasts and without fibroblasts using *InvasiCell*. Our data indicated that the secretion of collagen type III was increased at positions with fibroblasts and resulted in the formation of a stiff network (**Figure 27A**). However, we observed that in the absence of fibroblasts, the collagen seemed to accumulate near the core of the device, and the signal was significantly reduced (**Figure 27A and B**).

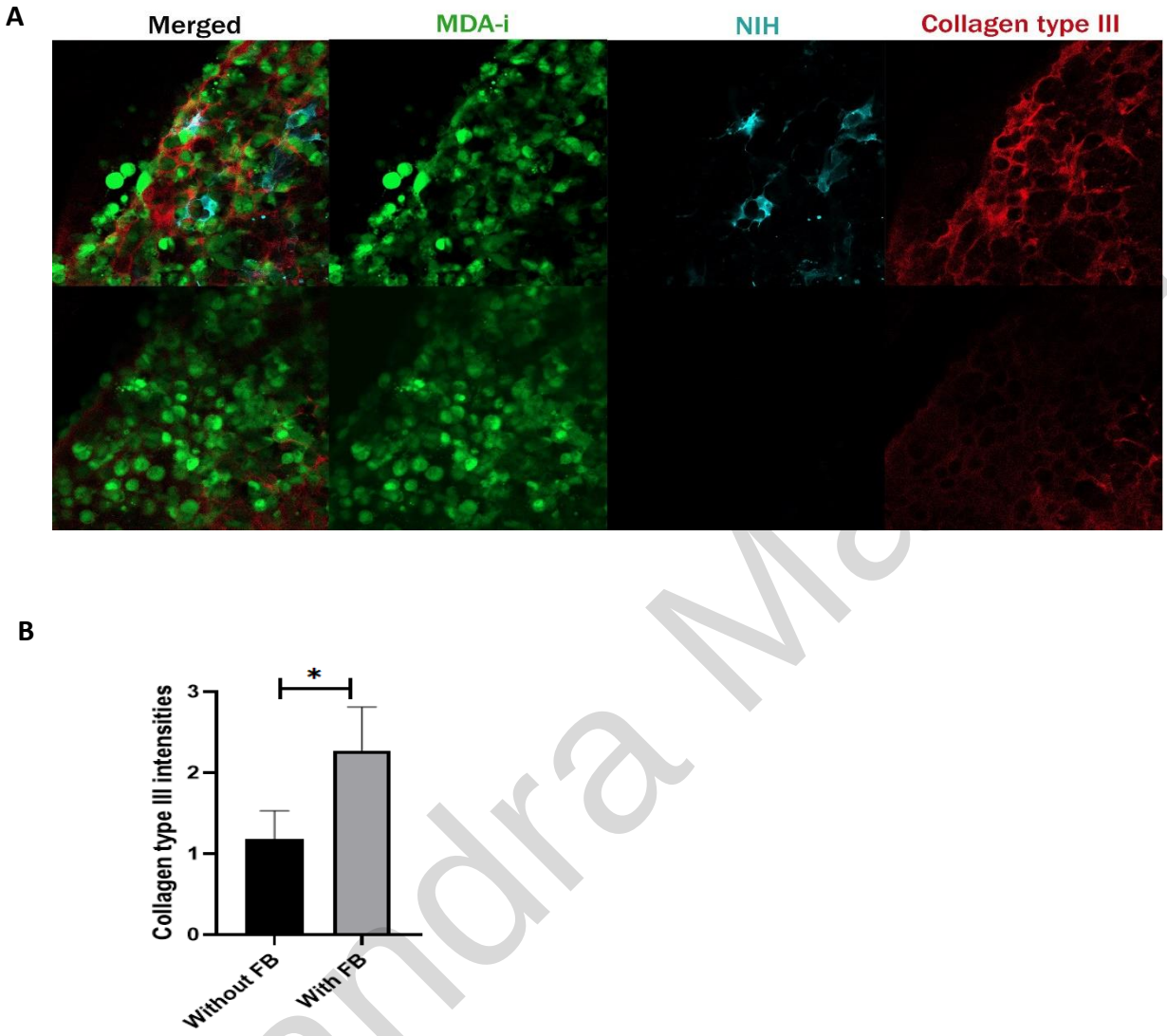

Figure 27: Immunofluorescent staining showed that the deposition of collagen type III is increased in the presence of fibroblasts. A) Confocal images of fixed invasion assays of MDA-i cells with and without fibroblasts (NIH) 5 days post their introduction into device. MDA-i cells are shown in green, and fibroblasts is shown with cyan. An antibody against collagen type III was used to detect its deposition, which is shown in red. **B)** Graphical representation of collagen type III fluorescence intensity without (black) and with fibroblasts (gray). The data were analyzed by two-tailed unpaired t-test, Data shown Mean ± S.D.

Furthermore, we conducted live imaging using invasion assays of tumor cells including fibroblasts in order to investigate the behavior of fibroblasts with tumor cells under conditions that exist in the tumor microenvironment. We observed that the fibroblasts that managed to exit from the core of the device displayed an elongated-shape morphology. In addition, our data showed that over time fibroblasts constantly assemble and disassemble multiple protrusions through which interact with tumor cells (**Figure 28**).

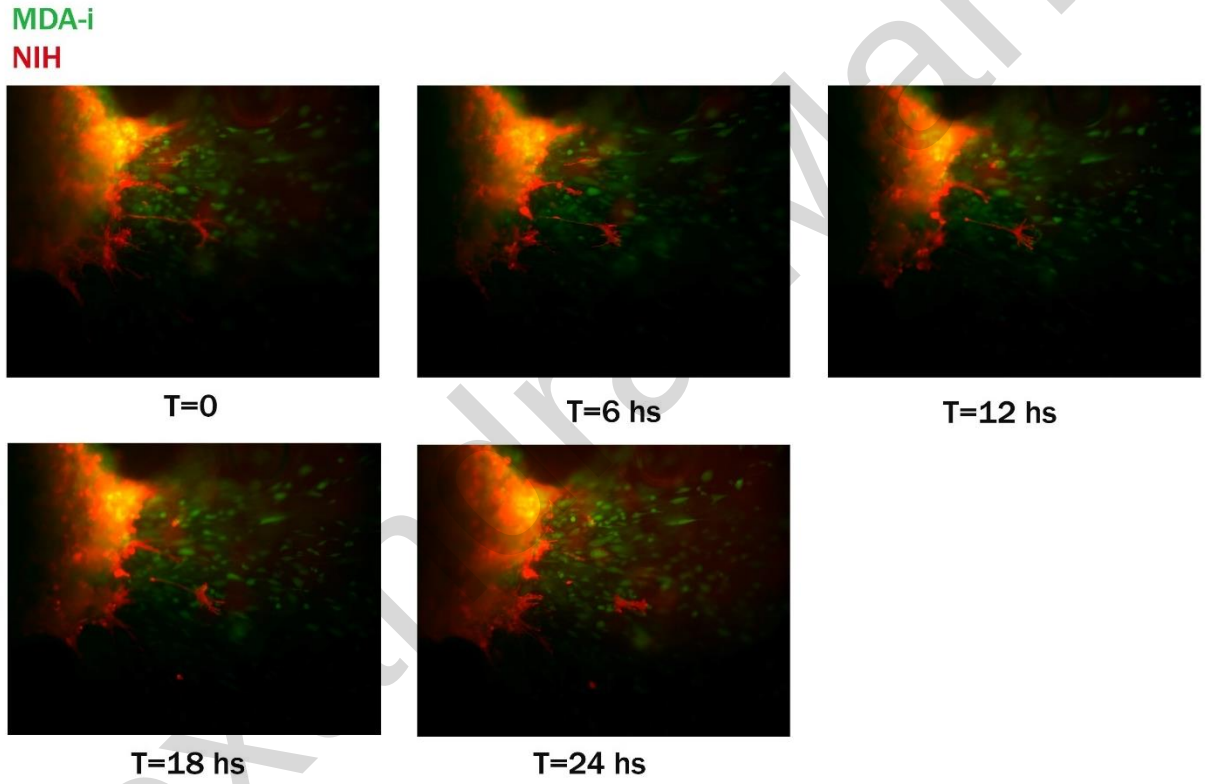

Figure 28: Fibroblasts interact with tumor cells by forming multiple protrusions. Fluorescent images from live imaging using invasion assays of MDA-i cells (green) with NIH fibroblasts (red), 3 days after introducing the cells into *InvasiCell*. The time point for each image is indicated below.

8.6 *InvasiCell* can be used to evaluate accurately cellular drug response compared to other *in vitro* assays

Several studies emphasized the need to develop new *in vitro* tools that mimic conditions existing in the tumor microenvironment leads to improve the efficiency of drug screenings (Hirata, 2017). Given that our data revealed that *InvasiCell* recapitulates the *in vivo* microenvironment, and the device can effectively reflect the different cell lines *in vivo* metastatic potential, we moved on to examine whether *InvasiCell* can be used as a drug response assay. Initially, MDA and MDA-i cells were treated with three different concentrations of Doxorubicin Hydrochloride under normal culturing conditions, in order to calculate the IC50 of the cells in response to the drug after 24 hours of treatment. Our data showed that a concentration of 43.76 μM of Doxorubicin Hydrochloride leads to the death of half of the cells, both for the MDA and MDA-i cell lines, after 24 hours (**Figure 29A)**. Subsequently, based on previously established for MDA cells in 3D tumor spheroids (Huang, 2020), *InvasiCell* devices were set up by using either the MDA or the MDA-i cell lines, and Doxorubicin Hydrochloride at a final concentration of 118.70 μM was introduced to the cell culturing media (**Figure 29B**). We used the fluorescence intensity as an indicator for the survival cell populations compared to the initials. Our results indicated that around 60% of the initial cells survived at this concentration after 24 hours of treatment. Additionally, we observed that after 72 hours of exposure to the drug, MDA-i cells showed significantly increased cell survival compared to their parental MDA cells within the *InvasiCell* (**Figure 29B**). Therefore, collected data suggested that cells showed enhanced drug resistance within the *InvasiCell* compared to tissue culture conditions. Also, in comparison with previous evaluations performed by Huang et al (Huang, 2020), cells within *InvasiCell* showed to be more resistant to potential medications compared to spheroids, as than the same cells in tumor spheroids, as Doxorubicin Hydrochloride IC50 tissue culture concentration by 2.713 folds in order to induce apoptosis to half of the cells within *InvasiCell*, whereas it had to only be increased by 1.356 folds to have the same effect in spheroids (**Figure 29 table**).

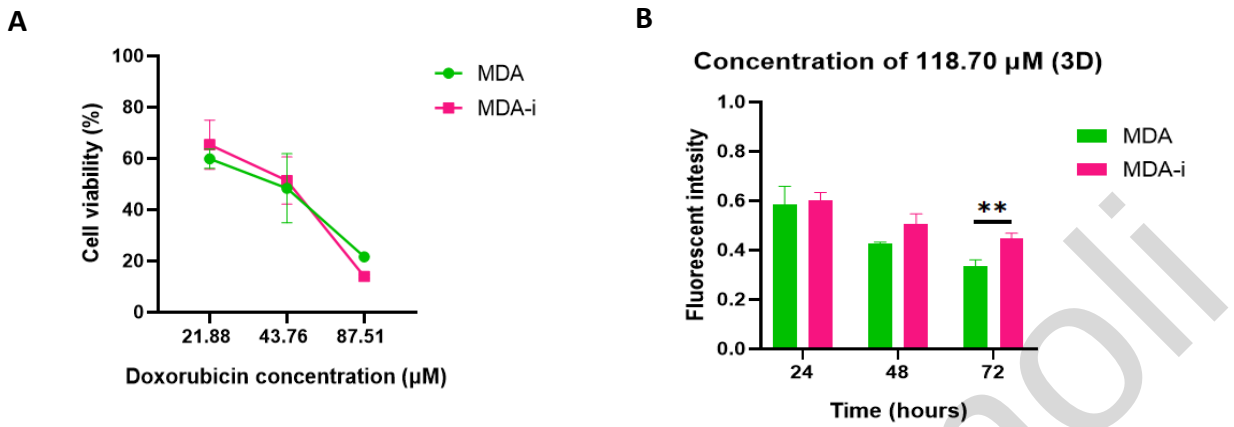

	IC50 values in 2D (µM)	IC50 values in 3D (µM)	Fold of increase in concentrations between 2D and 3D
Our experiments	43.76	118.70	2.713
Huang et al.	87.51	118.70	1.356

Figure 29: Evaluation of cellular response to Doxorubicin Hydrochloride using MDA and MDA-i cells under normal tissue culture conditions and within *InvasiCell*. A) Graphical representation of cell viability of MDA (green) and MDA-i (pink) after 24 hours of exposure to the drug concentration of 21.88 µM ,43.76 µM, and 87.51 µM in cell culture condition. **B)** Graphical representation of fluorescence intensity of MDA (green) and MDA-i (pink) after 24,48 and 72 hours of exposure to the drug concentration of 118.70 µM using *InvasiCell*. The fluorescence intensity is used as an indicator for the number of surviving cells. The data were normalized with the survival of untreated cells. Data shown as Mean ± S.D. The average was calculated using n=3 (each experiment for each concentration was performed in triplicate). A summary table illustrates the drug concentrations used in our experiments and those in the Huang et al. study under 2D tissue culture and 3D conditions using *InvasiCell* or spheroids respectively. The fold of increased in concentrations from 2D tissue culture to 3D conditions using *InvasiCell* or tumor spheroids respectively was calculated.

DISCUSSION

Cancer incidence has been increasing the past few decades making it the second leading cause of death worldwide. Metastasis is defined as the dissemination of tumor cells from primary tumor sites to secondary sites or distant organs. Approximately 90% of cancer-related deaths are attributed to metastasis (Lambert, 2017). Consequently, cancer research is undoubtedly important to provide knowledge about essential mechanisms of tumor progression and metastasis contributing to the development of new anti-cancer treatments. Both *in vivo* and *in vitro* tools used in cancer research have provided important insights about cancer progression. However, the main limitations of *in vitro* models used for cancer research can be summarized as the lack of reproducibility due to the absence of standardized protocols and the inability of most assays to replicate the *in vivo* tumor microenvironment which is crucial for both understanding cancer progression and evaluating the effectiveness of potential new therapies (Grada, 2017). These limitations of *in vitro* models were apparent in this study, which aimed to investigate whether *InvasiCell*, a novel in house build device, can be used as a physiologically relevant model to study various aspects of cancer progression compared to existing *in vitro* tools that are used in cancer research, such as the wound healing assays, Boyden chamber assays, and tumor spheroids.

9.1 Evaluation of the *in vitro* models used in cancer research

We initially performed the 2D wound healing assay which is one of the most commonly used assays in order to evaluate the migration abilities of tumor cells. However, it is known that wound healing assays are used to study the collective cell migration of normal and tumor cells under different experimental conditions (Migliaccio, 2023). According to the literature, the typical analysis of wound healing assays which is the estimation of migration abilities by the gap closure is appropriated for cell lines that undergo collective cell migration. Specifically, the gap closure must be measured by the “sheet” migration and not by tracking just an individual cell. This is because the migration abilities of cells in collective cell migration are influenced by cell-

to-cell interactions. (Javer, 2020) Thus, wound healing assays are not suitable for all cell types, and the examination of single-cell migration using wound healing assay requires altered analysis for accurate results (Riahi, 2012).

An additional limitation of wound healing assays is the variation in the gap between series of experiments. The scratching process caused cell damage resulting in the release of the cellular components and affecting the surrounding cells. Thus, studies demonstrated that differences in the extent of cell death because of the variation in gap size could have an impact on the migration capacities of cells (Guy, 2017). Furthermore, performing wound healing assays under starvation conditions is essential to eliminate the contribution of the proliferation factor to the gap closure. However, it has been suggested that starvation treatment needs specificity for each cell line regarding the concentration and duration (Zhao, 2020). Importantly wound healing assays fail to recapitulate any major conditions of the tumor microenvironment and their physiological relevance is further eroded by the fact that they measure 2D cell migration. Taking into account the inconsistency of wound healing data and the aforementioned limitations of these assays, makes it unlikely that they can reliably distinguish between cell lines with distinct in *vivo* metastatic potentials.

These limitations of the wound healing assay can be reflected in our findings, as they show that the wound healing method cannot reliably reflect the different metastatic potentials of cell lines. For instance, these assays failed to differentiate the non-metastatic breast MCF7 cells from the metastatic MDA and LM2 cells. In addition, wound healing assays were ineffective in discriminating the isolated pancreatic PANC-i cells from the parental PANC cells. As already mentioned, data from our lab demonstrated that the isolated PANC-i cells showed enhanced metastatic abilities than their parental PANC cells using zebrafish as *in vivo* model. It is interesting to note that wound healing was the only assay tested that failed to discriminate between MCF7, an epithelial cell line that retains tight junctions and cell lines that have undergone EMT such as MDA. We thus rank wound healing assays as the poorest choice for prediction of *in vivo* metastatic potential however this does not mean that the assay cannot be used to generate useful information as long as the researcher is aware of the limitations.

Similarly, the most commonly used assay to evaluate the metastatic potential of tumor cells is the Boyden chamber assays, which are also known as the transwell assays. Although the Boyden

chamber method is simple and widely used for studying cell migration and invasion, it does have some limitations. For instance, transwell migration assays are endpoint assays with poor reproducibility, and chamber inserts are expensive (Poon, 2022). In addition, it has been shown that the chemoattracts gradient generated are not maintained for more than a few hours (Isert, 2023). In an effort to enhance the sensitivity of Boyden chamber assays for examining the differentiation cells with different in vivo metastatic potentials, we performed modified Boyden chamber assays by adding an ECM barrier. However, our data revealed that the introduction of an ECM component into Boyden chamber assays does not remarkably enhance their ability to reflect the different *in vivo* metastatic potentials of cell lines. Furthermore, one challenge we faced by performing Modified Boyden chamber assays was the lack of a standardized protocol for modified Boyden chamber experiments. Particularly, we observed variations in the number of cells and in the time cells were allowed to invade between provided protocols for these assays. Moreover, there are two alternative ways to perform modified Boyden chamber experiments. Specifically, some scientists seed the examined cells on the top of the gel that mimics ECM, while others prefer to embed cells in the gel (Poon 2022, Gradiz 2016). Therefore, all these modifications observed in protocols could lead to different results. A standardization of the method would be very useful and allow more meaningful comparisons between published data.

For example, our data showed that only the non-metastatic MCF7 cell line was discriminated from the other breast metastatic cell lines by conducting Boyden chamber assays. This was an improvement over wound healing and stems from the inability of the epithelial cells to detach from their neighbors and pass through the pores. Additionally, these assays were unable to distinguish between other cell lines with significantly increased *in vivo* metastatic potentials such as LM2 from MDA, and isolated MDA-i and PANC-i from their parentals. As already mentioned, EMT is an essential process for tumor invasion and metastasis and is characterized by the switching of epithelial to mesenchymal expression markers. Furthermore, EMT has been associated with increased migration and invasion abilities that contribute to more aggressive phenotypes. Analysis of the breast cancer cell line demonstrated that the MCF7 cells showed epithelial characteristics while MDA cells displayed mesenchymal characteristics (Fenouille, 2012). Parallel studies in pancreatic cancer cell lines revealed that PACA and PANC cells express some epithelial and mesenchymal markers supporting that they undergo EMT (Dubois, 2017). According to these data, Boyden chamber assays failed to differentiate between cell lines

with distinct metastatic abilities and indirectly differentiated epithelial cells from those exhibiting acquired mesenchymal characteristics. Notably, scientists observed that the inhibition of EMT by promoting the expression of epithelial markers can reduce cell migration abilities using Boyden chamber assays (Sodek, 2009). These findings align with our data from Boyden chamber experiments where only the non-metastatic epithelial MCF7 cells showed significantly decreased migration abilities and were differentiated from the other metastatic breast cancer cell lines.

Based on our data showing that neither wound healing assays nor Boyden chamber assays could differentiate between cell lines with varying *in vivo* metastatic potential, we proceeded to perform tumor spheroids-based assays. It is generally accepted that 3D techniques are more physiologically relevant than 2D in vitro models and accurately resemble *in vivo* conditions. As mentioned previously, tumor spheroids are the gold standard 3D in vitro model to examine tumor progression, metastasis, and drug screening. Thus, we carried out tumor spheroid assays to investigate whether these assays could reflect the *in vivo* metastatic potentials of our examined cell lines. As reported extensively through the literature generating spheroids can be difficult for many tumor cell lines. Cells with low levels of cadherin receptors tend to be very challenging in this respect and indeed we were forced to establish and optimize the assay for our cell lines. Although tumor spheroid assays differentiated most of the cell lines for their *in vivo* metastatic potential, these assays failed to reflect the enhanced *in vivo* metastatic abilities of LM2 compared to MDA cells. Specifically, according to data from tumor spheroid assays, the MDA cells showed significantly elevated invasive potential than the LM2 cells which contrasts with their metastatic abilities observed *in vivo*. It has been demonstrated that MDA cells display reduced expression of E-cadherin and weak cell-to-cell interaction that contribute to their inability to form dense spheroids (Sutherland, 1988). It is possible that this is the reason MDA invade more in this assay. The TME conditions that are challenging and found in tight spheroids will most likely not be established in loose spheroids leading to elevated proliferation. Although various techniques have been developed for generating spheroids, even for cell lines such MDA which cannot form tightly adherent spheroids, these assays are challenging and time-consuming. In addition, several studies have reported that cells within compact spheroids exhibit altered cellular properties such as growth, invasiveness, sensitivity to drugs, and maintenance of spheroids structures including the necrotic core, due to the strong cell-to-cell communication (Han 2021,

Fernandez 2023). Thus, based on this, tumor spheroids methods may not be appropriate for examining all the cell types, because of the structure and morphology of spheroids affect the cellular properties (Fernandez, 2023).

Additional limitations of the tumor spheroids-based technique are the limited uniformity and reproducibility of tumor spheroids size and volume across multiple experiments even using the same protocol and cell type. Taking everything into account, tumor spheroids assays are considered unsuitable for performing high throughput drug evaluation testing anti-tumor medications (Fernandez, 2023).

Considering all of the above, the application of a 3D in vitro model remarkably enhances the accuracy of reflecting the *in vivo* metastatic abilities of our cell lines. However, tumor spheroids were ineffective to reflect the greater metastatic potential of LM2 than MDA cells.

9.2 Evaluation of *InvasiCell* as *in vitro* tool for cancer research

Unpublished data generated by Mr. Adonis Hajdigeorgiou revealed that *InvasiCell* can establish de novo gradients of nutrients, oxygen, pH and increased solid stress. These data suggest that *InvasiCell* can mimic conditions that exist in the tumor microenvironment. Additionally, it has been demonstrated that growing solid tumors generate three distinct regions including the necrotic core, the periphery ring, and the proliferative ring. Mr. Hajdigeorgiou's data showed that tumor spheroids generated by *InvasiCell* exhibit these three characteristic regions such as solid tumors in living organisms. Therefore, *InvasiCell* enables the examination of invasive potential of various cancer cell lines under a 3D environment that mimics *in vivo* situations without the addition of any equipment.

InvasiCell provides consistency in its protocol in contrast to other *in vitro* tools that lack standardized protocols. Specifically, the standardized protocol has been developed and validated by Mr. Hajdigeorgiou for studying invasive potential of various cancer cell types including breast, pancreatic and colorectal cancer cell lines. Thus, *InvasiCell* exhibits increased reproducibility compared to other in vitro tools used in cancer research. However, the set-up of *InvasiCell* display increased complexity compared to that of some other *in vitro* tools, such as the Boyden chamber assays which are the most commonly used in cancer research due to their

simplicity. Additionally, the time required to evaluate the invasion potential within *InvasiCell* can vary based on the invasion abilities of the examined cancer cell lines.

By performing invasion assays within the *InvasiCell*, we observed effective discrimination of all examined breast and pancreatic cell lines with varying *in vivo* metastatic potentials. Particularly, the non-metastatic MCF7 distinguished between the metastatic and highly metastatic MDA and LM2 cell lines respectively. Additionally, our data suggested that only *InvasiCell* was able to reflect the elevated metastatic abilities of LM2 compared to MDA. Furthermore, *InvasiCell* differentiates the device-isolated cell populations MDA-i and PANC-i from their respect parental cell lines. Therefore, collected data indicated that *InvasiCell* reflects the *in vivo* metastatic potential of evaluated cell lines more accurately and reliably than other *in vitro* models. **Figure 30** illustrates a summary table showing *the vitro* assays performed and their ability to reflect *in vivo* metastatic potential in various cell lines.

In vitro assay:	wound healing	Boyden chamber	Modified Boyden chamber	tumor spheroids	InvasiCell
Distinguishing between cells with varying in vivo metastatic potentials:	MDA/MDA-i Paca/Panc	MCF7	—	MCF7 MDA/MDA-i Paca/Panc Panc/Panc-i	MCF7/MDA/LM2 MDA/MDA-i Paca/Panc Panc/Panc-i
Difficulties in distinguishing cells with varying in vivo metastatic potentials:	MCF7/MDA/LM2 Panc/Panc-i	MDA/LM2 MDA/MDA-i Paca/Panc Panc/Panc-i	MDA/MDA-i Panc/Panc-i	MDA/LM2	—

Figure 30: Summary table of data collected by performing several in vitro assays. The table shows all the in vitro assays performed (wound healing assays, Boyden chamber assays, modified Boyden chamber assays and tumor spheroids) and their ability to reflect the varying in vivo metastatic potentials of examined cell lines.

9.3 Introduction of fibroblasts within *InvasiCell*

In addition, *InvasiCell* allows researcher to carry out co-culture experiments with other cell types existing in the tumor microenvironment and study cellular interactions, due to its flexible set up protocol. Our data showed that the inclusion of NIH3T3 fibroblasts in the core of the device with tumor cells caused a reduction in the invasive potential of the tumor cells compared to their invasion rates in the absence of fibroblasts. According to the literature, some key functions of fibroblasts in the tumor microenvironment are the remodeling of ECM and altering the stiffness by secretion of ECM components including Lamins, collagen, and fibronectin (Hirayama, 2017). Our data for immunofluorescence staining revealed that the deposition of collagen type III was significantly increased in the presence of fibroblasts compared to invasion assays without fibroblasts. One of the reasons that caused the reduction in invasive potentials of tumor cells could be the enhanced stiffness gels because of the increased collagen secretion by fibroblasts. Additionally, via time-lapse imaging, we observed that tumor cells displayed physical interactions with fibroblasts during their invasion. This also can contribute to the delay in the invasive potential of tumor cells due to the relatively low motility of fibroblasts. Furthermore, only a small number of fibroblasts manage to survive in the environment provided by *InvasiCell*, which increases cell toxicity and affects the properties of tumor cells due to the harsh environmental conditions. Finally, the release of growth factors and other signaling molecules from fibroblasts in the tumor microenvironment was found to influence the tumor cell behavior (Feng, 2022). Hence it could be an additional explanation for the delayed invasive abilities exhibited by tumor cells. It should be noted that these experiments were carried out through the introduction of fibroblasts not CAFs in the device. We have shown that these cells effectively turn into CAFs however this process is slow and these experiments should ideally be repeated using CAFs which presumably will have an improved capacity to survive the harsh conditions in the core but in addition could impact their ability to modulate the invasive capacity of tumor cells.

9.4 Drug response within *InvasiCell*

Our last question was to examine whether the *InvasiCell* can be used as a valid tool for drug response. Our data indicated that tumor cells within the *InvasiCell* showed enhanced drug resistance in Doxorubicin hydrochloride relative to normal tissue culture conditions. These findings resemble previously published studies performed with spheroid assays (Huang, 2020). However, we observed that the magnitude of concentration changes between tissue culture and *InvasiCell* is greater than used between tissue culture and spheroids in other studies. Thus, *InvasiCell* can provide a more accurate evaluation of cellular drug responses to different drugs compared to other *in vitro* tools.

9.5 Conclusion

In conclusion, *InvasiCell* reflects the *in vivo* metastatic abilities of cell lines more accurately than any other widely used in vitro tools including wound healing assays, Boyden chamber assays, modified Boyden chamber assays and tumor spheroids. Additionally, the device enables the study of cellular interaction between tumor cells and other cell types present in the tumor microenvironment and the examination of cellular responses to different drugs. Therefore, *InvasiCell* is a promising *in vitro* tool that could enhance our understanding of tumor progression and evaluate potential anti-tumor therapies more reliably than existing *in vitro* assays.

Moreover, *in vivo* models are considered the ideal tool for studying various aspects of cancer such as metastasis, however, they display significant limitations. It has been reported that orthotopic injections are recommended over subcutaneous injections for evaluating the metastatic potential of pancreatic ductal adenocarcinoma. However, scientists demonstrated that orthotopic models have technical difficulties such as the challenging injection site and requirement of specific equipment for observing tumor growth due to the limited accessibility (Fernandez, 2023). Therefore, *InvasiCell* could be used along with in vivo experiments to eliminate some of the technical challenges associated with evaluating the metastatic potential of certain cell lines using orthotopic mice injections.

9.6 Future experiments:

Studies demonstrated that the CAFs derived from varying sources of the tumor microenvironment however they primarily originated from resting present in the tumor site (Feng, 2022). Future experiments will be focused on investigating whether other subtypes of fibroblasts such as human mammary fibroblast (HMF), which is isolated from human breast, could impact the invasive potential of tumor cell lines differently compared to results observed using the embryonic NIH3T3 fibroblasts. Thus, we will perform invasion assays including different types of fibroblasts along with the tumor cells in the core of *InvasiCell* and we will examine the invasiveness of tumor cell lines. Furthermore, Immunofluorescence staining for additional ECM components such as Lamin and Fibronectin could be performed for further investigation of ECM remodeling due to the presence of fibroblasts. Additionally, it is known that one of the mechanisms for activating and transforming normal residual fibroblasts into CAFs is the contact-dependent signaling mediated by the interaction with tumor cells (Feng, 2022). Based on that, future experiments will be performed using co-culture experiments between tumor cells and fibroblasts under in vivo conditions including starvation, hypoxia, and acidosis. After allowing sufficient time for CAF formation, we will repeat the experiments with the inclusion of fibroblasts in the core of *InvasiCell* within tumor cells, to examine cellular interaction and the invasive potential of tumor cells.

In order to evaluate further the cellular drug response provided by *InvasiCell*, additional concentrations of Doxorubicin hydrochloride will be tested in invasion assays using breast cancer cells lines. In addition, all experiments performed with Doxorubicin hydrochloride will be repeated using the pancreatic cancer cell lines to examine potential differences in cellular drug responses between breast and pancreatic cancer cell lines under normal tissue culture conditions and within *InvasiCell*. Eventually, similar experiments will be conducted using alternative anti-tumor medications that are used in cancer research, such as Cisplatin, to evaluate the cellular drug responses using the *InvasiCell*.

ABBREVIATIONS

ABBREVIATION	MEANING
EMT	Epithelial to mesenchymal transition
MAT	Mesenchymal to amoeboid transition
CAT	Collective to amoeboid transition
ECM	Extracellular matrix
MET	Mesenchymal to epithelial transition
TME	Tumor microenvironment
CAFs	Cancer associated fibroblasts
TAMs	Tumor associated macrophages
HIFs	Hypoxia-inducible factors
ATP	Adenosine triphosphate
VEGF	Vascular endothelial growth factor
α-SMA	α-Smooth muscle actin
FSP	Fibroblast specific protein
PDGF	Platelet-derived growth factor
EndMET	Endothelial to mesenchymal transition

TGF-β	Transforming growth factor beta
STAT3	Signal transducer and activator of transcription 3
FA	Focal Adhesions
MDA	MDA-MB-231
LM2	MDA-231-LM2-4175
PACA	MIA PaCa-2
PANC	PANC-1
IC50	Half-maximal inhibitory concentration

BIBLIOGRAPHY

. Available: https://www.who.int/news-room/fact-sheets/detail/cancer [Accessed 19 May 2024].

. Available: https://www.cancerresearchuk.org/about-cancer/what-is-cancer/how-cancer-starts/types-of-cancer [Accessed 19 May 2024].

. Available: https://training.seer.cancer.gov/disease/categories/classification.html [Accessed 19 May 2024].

. Available: https://www.thermofisher.com/cy/en/home/life-science/cancer-research/solid-tumor-research.html [Accessed 19 May 2024].

. Available: https://www.cancer.gov/types/metastatic-cancer [Accessed 19 May 2024].

. Available: https://www.wcrf.org/cancer-trends/breast-cancer-statistics/ [Accessed 19 May 2024].

AHMADIANKIA, N., MOGHADDAM, H. K., MISHAN, M. A., BAHRAMI, A. R., NADERI-MESHKIN, H., BIDKHORI, H. R., MOGHADDAM, M. & MIRFEYZI, S. J. 2016. Berberine suppresses migration of MCF-7 breast cancer cells through down-regulation of chemokine receptors. *Iran J Basic Med Sci*, 19, 125-31.

ALEXANDRA, M. 2022. Selection pressure within the InvasiCell Device leads to gene expression changes which result in more aggressive tumor cell populations. Biological Science, University of Cyprus.

ANDERSON, N. M. & SIMON, M. C. 2020. The tumor microenvironment. *Curr Biol*, 30, R921-r925.

ANDREUCCI, E., FIORETTO, B. S., ROSA, I., MATUCCI-CERINIC, M., BIAGIONI, A., ROMANO, E., CALORINI, L. & MANETTI, M. 2023. Extracellular Lactic Acidosis of the Tumor Microenvironment Drives Adipocyte-to-Myofibroblast Transition Fueling the Generation of Cancer-Associated Fibroblasts. *Cells*, 12.

AZADI, S., ABOULKHEYR ES, H., KULASINGHE, A., BORDHAN, P. & EBRAHIMI WARKIANI, M. 2020. Chapter Five - Application of microfluidic technology in cancer research and therapy. In: MAKOWSKI, G. S. (ed.) *Advances in Clinical Chemistry*. Elsevier.

BAGHBAN, R., ROSHANGAR, L., JAHANBAN-ESFAHLAN, R., SEIDI, K., EBRAHIMI-KALAN, A., JAYMAND, M., KOLAHIAN, S., JAVAHERI, T. & ZARE, P. 2020. Tumor microenvironment complexity and therapeutic implications at a glance. *Cell Communication and Signaling*, 18, 59.

BARGAHI, N., GHASEMALI, S., JAHANDAR-LASHAKI, S. & NAZARI, A. 2022. Recent advances for cancer detection and treatment by microfluidic technology, review and update. *Biological Procedures Online*, 24, 5.

BENSINGER, S. J. & CHRISTOFK, H. R. 2012. New aspects of the Warburg effect in cancer cell biology. *Seminars in Cell & Developmental Biology*, 23, 352-361.

BIED, M., HO, W. W., GINHOUX, F. & BLÉRIOT, C. 2023. Roles of macrophages in tumor development: a spatiotemporal perspective. *Cellular & Molecular Immunology*, 20, 983-992.
BISE, R., KANADE, T., YIN, Z., HUH, S. J. A. I. C. O. T. I. E. I. M. & SOCIETY, B. 2011. Automatic cell tracking applied to analysis of cell migration in wound healing assay. 6174-6179.

CAIRNS, R., PAPANDREOU, I. & DENKO, N. 2006. Overcoming Physiologic Barriers to Cancer Treatment by Molecularly Targeting the Tumor Microenvironment. *Molecular Cancer Research*, 4, 61-70.

CAIRNS, R., PAPANDREOU, I. & DENKO, N. 2006. Overcoming Physiologic Barriers to Cancer Treatment by Molecularly Targeting the Tumor Microenvironment. *Molecular Cancer Research*, 4, 61-70.

CAMPANALE, J. P. & MONTELL, D. J. 2023. Who's really in charge: Diverse follower cell behaviors in collective cell migration. *Current Opinion in Cell Biology*, 81, 102160.

CAO, Z.-Q., WANG, Z. & LENG, P. 2019. Aberrant N-cadherin expression in cancer. *Biomedicine & Pharmacotherapy*, 118, 109320.

CHANDRA, P. K., DATTA, A. & MONDAL, D. 2020. Chapter 5 - Development of mouse models for cancer research. In: VERMA, A. S. & SINGH, A. (eds.) Animal Biotechnology (Second Edition). Boston: Academic Press.

CHAPNICK, D. A. & LIU, X. 2014. Leader cell positioning drives wound-directed collective migration in TGFβ-stimulated epithelial sheets. Mol Biol Cell, 25, 1586-93.

CHEN, X. & SONG, E. 2019. Turning foes to friends: targeting cancer-associated fibroblasts. *Nature Reviews Drug Discovery*, 18, 99-115.

CHRISTENSEN, S. T., VELAND, I. R., SCHWAB, A., CAMMER, M. & SATIR, P. 2013. Chapter Three - Analysis of Primary Cilia in Directional Cell Migration in Fibroblasts. In: MARSHALL, W. F. (ed.) Methods in Enzymology. Academic Press.

CHRISTIANSEN, J. J. & RAJASEKARAN, A. K. 2006. Reassessing Epithelial to Mesenchymal Transition as a Prerequisite for Carcinoma Invasion and Metastasis. *Cancer Research*, 66, 8319-8326.

CIRRI, P. & CHIARUGI, P. 2011. Cancer associated fibroblasts: the dark side of the coin. *Am J Cancer Res*, 1, 482-97.

CONNER, S. J., GUARIN, J. R., LE, T. T., FATHERREE, J. P., KELLEY, C., PAYNE, S. L., PARKER, S. R., BLOOMER, H., ZHANG, C., SALHANY, K., MCGINN, R. A., HENRICH, E., YUI, A., SRINIVASAN, D., BORGES, H. & OUDIN, M. J. 2024. Cell morphology best predicts tumorigenicity and metastasis in vivo across multiple TNBC cell lines of different metastatic potential. *Breast Cancer Res*, 26, 43.

COURTNAY, R., NGO, D. C., MALIK, N., VERVERIS, K., TORTORELLA, S. M. & KARAGIANNIS, T. C. 2015. Cancer metabolism and the Warburg effect: the role of HIF-1 and PI3K. *Molecular Biology Reports*, 42, 841-851.

DA CUNHA, B. R., DOMINGOS, C., STEFANINI, A. C. B., HENRIQUE, T., POLACHINI, G. M., CASTELO-BRANCO, P. & TAJARA, E. H. 2019. Cellular Interactions in the Tumor Microenvironment: The Role of Secretome. *J Cancer*, 10, 4574-4587.

DOUGLAS HANAHAN1, * AND ROBERT A. WEINBERG3,* 2011. Hallmarks of Cancer: The Next Generation. *Cell*.

DU, Y., LIU, Z., YOU, L., HOU, P., REN, X., JIAO, T., ZHAO, W., LI, Z., SHU, H., LIU, C. & ZHAO, Y. 2017. Pancreatic Cancer Progression Relies upon Mutant p53-Induced Oncogenic Signaling Mediated by NOP14. *Cancer Research*, 77, 2661-2673.

DUBOIS, C., DUFOUR, R., DAUMAR, P., AUBEL, C., SZCZEPANIAK, C., BLAVIGNAC, C., MOUNETOU, E., PENAULT-LLORCA, F. & BAMDAD, M. 2017. Development and cytotoxic response of two proliferative MDA-MB-231 and non-proliferative SUM1315 three-dimensional cell culture models of triple-negative basal-like breast cancer cell lines. *Oncotarget*, 8, 95316-95331.

ESTRELLA, V., CHEN, T., LLOYD, M., WOJTKOWIAK, J., CORNNELL, H. H., IBRAHIM-HASHIM, A., BAILEY, K., BALAGURUNATHAN, Y., ROTHBERG, J. M., SLOANE, B. F., JOHNSON, J., GATENBY, R. A. & GILLIES, R. J. 2013. Acidity Generated by the Tumor Microenvironment Drives Local Invasion. *Cancer Research*, 73, 1524-1535.
FENG, B., WU, J., SHEN, B., JIANG, F. & FENG, J. 2022. Cancer-associated fibroblasts and resistance to anticancer therapies: status, mechanisms, and countermeasures. *Cancer Cell International*, 22, 166.

FENOUILLE, N., TICHET, M., DUFIES, M., POTTIER, A., MOGHA, A., SOO, J. K., ROCCHI, S., MALLAVIALLE, A., GALIBERT, M.-D., KHAMMARI, A., LACOUR, J.-P., BALLOTTI, R., DECKERT, M. & TARTARE-DECKERT, S. 2012. The Epithelial-Mesenchymal Transition (EMT) Regulatory Factor SLUG (SNAI2) Is a Downstream Target of SPARC and AKT in Promoting Melanoma Cell Invasion. *PLOS ONE*, 7, e40378.

FERNANDEZ, J. L., ÅRBOGEN, S., SADEGHINIA, M. J., HARAM, M., SNIPSTAD, S., TORP, S. H., EINEN, C., MÜHLENPFORDT, M., MAARDALEN, M., VIKEDAL, K. & DAVIES, C. D. L. 2023. A Comparative Analysis of Orthotopic and Subcutaneous Pancreatic Tumour Models: *Tumour Microenvironment and Drug Delivery*. 15, 5415.

FRIEDL, P. & GILMOUR, D. 2009. Collective cell migration in morphogenesis, regeneration and cancer. *Nature Reviews Molecular Cell Biology*, 10, 445-457.

GANDAGLIA, G., KARAKIEWICZ, P. I., BRIGANTI, A., PASSONI, N. M., SCHIFFMANN, J., TRUDEAU, V., GRAEFEN, M., MONTORSI, F. & SUN, M. 2015. Impact of the Site of Metastases on Survival in Patients with Metastatic Prostate Cancer. *European Urology*, 68, 325-334.

GHEYTANCHI, E., NASERI, M., KARIMI-BUSHERI, F., ATYABI, F., MIRSHARIF, E. S., BOZORGMEHR, M., GHODS, R. & MADJD, Z. 2021. Morphological and molecular characteristics of spheroid formation in HT-29 and Caco-2 colorectal cancer cell lines. *Cancer Cell International*, 21, 204.

GONG, X., LIN, C., CHENG, J., SU, J., ZHAO, H., LIU, T., WEN, X. & ZHAO, P. 2015. Generation of Multicellular Tumor Spheroids with Microwell-Based Agarose Scaffolds for Drug Testing. PLOS ONE, 10, e0130348.

GOV, N. S. 2007. Collective cell migration patterns: follow the leader. *Proc Natl Acad Sci U S A*, 104, 15970-1.

GRADA, A., OTERO-VINAS, M., PRIETO-CASTRILLO, F., OBAGI, Z. & FALANGA, V. 2017. Research Techniques Made Simple: Analysis of Collective Cell Migration Using the Wound Healing Assay. *J Invest Dermatol*, 137, e11-e16.

GRADA, A., OTERO-VINAS, M., PRIETO-CASTRILLO, F., OBAGI, Z. & FALANGA, V. 2017. Research Techniques Made Simple: Analysis of Collective Cell Migration Using the Wound Healing Assay. *Journal of Investigative Dermatology*, 137, e11-e16.

GRADIZ, R., SILVA, H. C., CARVALHO, L., BOTELHO, M. F. & MOTA-PINTO, A. 2016. MIA PaCa-2 and PANC-1 - pancreas ductal adenocarcinoma cell lines with neuroendocrine differentiation and somatostatin receptors. *Sci Rep*, 6, 21648.

GRADIZ, R., SILVA, H. C., CARVALHO, L., BOTELHO, M. F. & MOTA-PINTO, A. 2016. MIA PaCa-2 and PANC-1 - pancreas ductal adenocarcinoma cell lines with neuroendocrine differentiation and somatostatin receptors. *Sci Rep*, 6, 21648.

GUY, J. B., ESPENEL, S., VALLARD, A., BATTISTON-MONTAGNE, P., WOZNY, A. S., ARDAIL, D., ALPHONSE, G., RANCOULE, C., RODRIGUEZ-LAFRASSE, C. & MAGNE, N. 2017. Evaluation of the Cell Invasion and Migration Process: A Comparison of the Video Microscope-based Scratch Wound Assay and the Boyden Chamber Assay. *J Vis Exp*.

HAN, S. J., KWON, S. & KIM, K. S. 2021. Challenges of applying multicellular tumor spheroids in preclinical phase. *Cancer Cell International*, 21, 152.

HAN, X., XU, X., YANG, C. & LIU, G. 2023. Microfluidic design in single-cell sequencing and application to cancer precision medicine. *Cell Rep Methods*, 3, 100591.

HAPACH, L. A., MOSIER, J. A., WANG, W. & REINHART-KING, C. A. 2019. Engineered models to parse apart the metastatic cascade. *npj Precision Oncology*, 3, 20.

HELDIN, C.-H., RUBIN, K., PIETRAS, K. & ÖSTMAN, A. 2004. High interstitial fluid pressure — an obstacle in cancer therapy. *Nature Reviews Cancer*, 4, 806-813.

HINZ, B., PHAN, S. H., THANNICKAL, V. J., GALLI, A., BOCHATON-PIALLAT, M. L. & GABBIANI, G. 2007. The myofibroblast: one function, multiple origins. *Am J Pathol*, 170, 1807-16.

HIRATA, E. & SAHAI, E. 2017. Tumor Microenvironment and Differential Responses to Therapy. Cold Spring Harb Perspect Med, 7.

HIRAYAMA, D., IIDA, T. & NAKASE, H. 2017. The Phagocytic Function of Macrophage-Enforcing Innate Immunity and Tissue Homeostasis. *Int J Mol Sci*, 19.

HUANG, Z., YU, P. & TANG, J. 2020. Characterization of Triple-Negative Breast Cancer MDA-MB-231 Cell Spheroid Model. *Onco Targets Ther*, 13, 5395-5405.

ISERT, L., MEHTA, A., LOIUDICE, G., OLIVA, A., ROIDL, A. & MERKEL, O. M. 2023. An In Vitro Approach to Model EMT in Breast Cancer. *Int J Mol Sci*, 24.

JARDIM, D. L., GROVES, E. S., BREITFELD, P. P. & KURZROCK, R. 2017. Factors associated with failure of oncology drugs in late-stage clinical development: A systematic review. *Cancer Treat Rev*, 52, 12-21.

JAVER, A., RITTSCHER, J. & SAILEM, H. Z. 2020. DeepScratch: Single-cell based topological metrics of scratch wound assays. *Computational and Structural Biotechnology Journal*, 18, 2501-2509.

JUBELIN, C., MUÑOZ-GARCIA, J., GRISCOM, L., COCHONNEAU, D., OLLIVIER, E., HEYMANN, M.-F., VALLETTE, F. M., OLIVER, L. & HEYMANN, D. 2022. Three-dimensional in vitro culture models in oncology research. *Cell & Bioscience*, 12, 155.

JUSTUS, C. R., MARIE, M. A., SANDERLIN, E. J. & YANG, L. V. 2023. Transwell In Vitro Cell Migration and Invasion Assays. In: FRIEDRICH, O. & GILBERT, D. F. (eds.) Cell Viability Assays: Methods and Protocols. New York, NY: Springer US.

KALLURI, R. & WEINBERG, R. A. 2009. The basics of epithelial-mesenchymal transition. *J Clin Invest*, 119, 1420-8.

KASZAK, I., WITKOWSKA-PIŁASZEWICZ, O., NIEWIADOMSKA, Z., DWORECKA-KASZAK, B., NGOSA TOKA, F. & JURKA, P. 2020. Role of Cadherins in Cancer-A Review. *Int J Mol Sci*, 21.

KATT, M. E., PLACONE, A. L., WONG, A. D., XU, Z. S. & SEARSON, P. C. 2016. In Vitro Tumor Models: Advantages, Disadvantages, Variables, and Selecting the Right Platform. 4.

KIM, S.-A., LEE, E. K. & KUH, H.-J. 2015. Co-culture of 3D tumor spheroids with fibroblasts as a model for epithelial–mesenchymal transition in vitro. *Experimental Cell Research*, 335, 187-196.

KIM, S.-J., KHADKA, D. & SEO, J. H. 2022. Interplay between Solid Tumors and Tumor *Microenvironment*. 13.

KIM, S. K. & CHO, S. W. 2022. The Evasion Mechanisms of Cancer Immunity and Drug Intervention in the Tumor Microenvironment. *Front Pharmacol*, 13, 868695.

KRAKHMAL, N. V., ZAVYALOVA, M. V., DENISOV, E. V., VTORUSHIN, S. V. & PERELMUTER, V. M. 2015. Cancer Invasion: Patterns and Mechanisms. *Acta Naturae*, 7, 17-28.

KRAMER, N., WALZL, A., UNGER, C., ROSNER, M., KRUPITZA, G., HENGSTSCHLÄGER, M. & DOLZNIG, H. 2013. In vitro cell migration and invasion assays. *Mutation Research/Reviews in Mutation Research*, 752, 10-24.

LAMBERT, A. W., PATTABIRAMAN, D. R. & WEINBERG, R. A. 2017. Emerging Biological Principles of Metastasis. *Cell*, 168, 670-691.

LANGHANS, S. A. 2018. Three-Dimensional in Vitro Cell Culture Models in Drug Discovery and Drug Repositioning. 9.

LEE, J.-W., BAE, S.-H., JEONG, J.-W., KIM, S.-H. & KIM, K.-W. 2004. Hypoxia-inducible factor (HIF-1)α: its protein stability and biological functions. *Experimental & Molecular Medicine*, 36, 1-12.

LENDECKEL, U., VENZ, S. & WOLKE, C. 2022. Macrophages: shapes and functions. *ChemTexts*, 8, 12.

LI, Y., ZHAO, L. & LI, X. F. 2021. Hypoxia and the Tumor Microenvironment. Technol *Cancer Res Treat*, 20, 15330338211036304.

LIN, Y., XU, J. & LAN, H. 2019. Tumor-associated macrophages in tumor metastasis: biological roles and clinical therapeutic applications. *Journal of Hematology & Oncology*, 12, 76.

LUTZ, W. K. & FEKETE, T. 1996. Endogenous and exogenous factors in carcinogenesis: limits to cancer prevention. *International Archives of Occupational and Environmental Health*, 68, 120-125.

MAHALMANI, V., SINHA, S., PRAKASH, A. & MEDHI, B. 2022. Translational research: Bridging the gap between preclinical and clinical research. *Indian J Pharmacol*, 54, 393-396.

MALINOVA, T. S. & HUVENEERS, S. 2018. Sensing of Cytoskeletal Forces by Asymmetric Adherens Junctions. *Trends in Cell Biology*, 28, 328-341.

MANDUCA, N., MACCAFEO, E., DE MARIA, R., SISTIGU, A. & MUSELLA, M. 2023. 3D cancer models: One step closer to in vitro human studies. 14.

MARTINEZ-PACHECO, S. & O'DRISCOLL, L. 2021. Pre-Clinical In Vitro Models Used in Cancer Research: Results of a Worldwide Survey. *Cancers (Basel*), 13.

MEHRABI, M., AMINI, F. & MEHRABI, S. 2018. Active Role of the Necrotic Zone in Desensitization of Hypoxic Macrophages and Regulation of CSC-Fate: A hypothesis. Front *Oncol*, 8, 235.

MIGLIACCIO, G., FERRARO, R., WANG, Z., CRISTINI, V., DOGRA, P. & CASERTA, S. 2023. Exploring Cell Migration Mechanisms in Cancer: From Wound Healing Assays to Cellular Automata Models. *Cancers (Basel),* 15.

MIGLIACCIO, G., FERRARO, R., WANG, Z., CRISTINI, V., DOGRA, P. & CASERTA, S. 2023. Exploring Cell Migration Mechanisms in Cancer: From Wound Healing Assays to Cellular Automata Models. 15, 5284.

MROZIK, K. M., BLASCHUK, O. W., CHEONG, C. M., ZANNETTINO, A. C. W. & VANDYKE, K. 2018. N-cadherin in cancer metastasis, its emerging role in haematological malignancies and potential as a therapeutic target in cancer. BMC *Cancer*, 18, 939.

OH, Y., TAYLOR, S., BEKELE, B. N., DEBNAM, J. M., ALLEN, P. K., SUKI, D., SAWAYA, R., KOMAKI, R., STEWART, D. J. & KARP, D. D. 2009. Number of metastatic sites is a strong predictor of survival in patients with nonsmall cell lung cancer with or without brain metastases. *Cancer*, 115, 2930-8.

PAN, Y., YU, Y., WANG, X. & ZHANG, T. 2020. Tumor-Associated Macrophages in Tumor Immunity. *Front Immunol*, 11, 583084.

PECORINO, L. Molecular Biology of Cancer: Mechanisms, Targets, and Therapeutics.

PEINADO, H., OLMEDA, D. & CANO, A. 2007. Snail, Zeb and bHLH factors in tumour progression: an alliance against the epithelial phenotype? *Nature Reviews Cancer*, 7, 415-428.

PERNOT, S., EVRARD, S. & KHATIB, A. M. 2022. The Give-and-Take Interaction Between the Tumor Microenvironment and Immune Cells Regulating Tumor Progression and Repression. *Front Immunol*, 13, 850856.

PILLAI, S. R., DAMAGHI, M., MARUNAKA, Y., SPUGNINI, E. P., FAIS, S. & GILLIES, R. J. 2019. Causes, consequences, and therapy of tumors acidosis. *Cancer Metastasis Rev*, 38, 205-222.

POON, S. & AILLES, L. E. 2022. Modeling the Role of Cancer-Associated Fibroblasts in Tumor Cell Invasion. 14, 962.

QIN, L., YANG, D., YI, W., CAO, H. & XIAO, G. 2021. Roles of leader and follower cells in collective cell migration. *Mol Biol Cell,* 32, 1267-1272.

RIAHI, R., YANG, Y., ZHANG, D. D. & WONG, P. K. 2012. Advances in Wound-Healing Assays for Probing Collective Cell Migration. *SLAS Technology*, 17, 59-65.

RIGOULET, M., BOUCHEZ, C. L., PAUMARD, P., RANSAC, S., CUVELLIER, S., DUVEZIN-CAUBET, S., MAZAT, J. P. & DEVIN, A. 2020. Cell energy metabolism: An update. Biochimica et Biophysica Acta (BBA) - *Bioenergetics*, 1861, 148276.

RIIHIMÄKI, M., HEMMINKI, A., FALLAH, M., THOMSEN, H., SUNDQUIST, K., SUNDQUIST, J. & HEMMINKI, K. 2014. Metastatic sites and survival in lung cancer. *Lung Cancer*, 86, 78-84.

SAFA, A. R. 2020. Epithelial-mesenchymal transition: a hallmark in pancreatic cancer stem cell migration, metastasis formation, and drug resistance. *J Cancer Metastasis Treat*, 6.

SANTIAGO-MEDINA, M., PALMER, T. & YANG, J. 2016. Cancer Cell Invasion through Tissue Barriers. In: BRADSHAW, R. A. & STAHL, P. D. (eds.) Encyclopedia of Cell Biology. Waltham: Academic Press.

SCHIRMER, U., SCHNEIDER, S. A., KHROMOV, T., BREMMER, F., SCHMINKE, B., SCHLIEPHAKE, H., LIEFEITH, K. & BROCKMEYER, P. 2024. Sclerostin Alters Tumor Cell Characteristics of Oral Squamous Cell Carcinoma and May Be a Key Player in Local Bone Invasion. 13, 137.

SENSI, F., D'ANGELO, E., D'ARONCO, S., MOLINARO, R. & AGOSTINI, M. 2019. Preclinical three-dimensional colorectal cancer model: The next generation of in vitro drug efficacy evaluation. 234, 181-191.

SHAMIR, E. R. & EWALD, A. J. 2014. Three-dimensional organotypic culture: experimental models of mammalian biology and disease. *Nature Reviews Molecular Cell Biology*, 15, 647-664.

SODEK, K. L., RINGUETTE, M. J. & BROWN, T. J. 2009. Compact spheroid formation by ovarian cancer cells is associated with contractile behavior and an invasive phenotype. *Int J Cancer*, 124, 2060-70.

SPILL, F., REYNOLDS, D. S., KAMM, R. D. & ZAMAN, M. H. 2016. Impact of the physical microenvironment on tumor progression and metastasis. *Curr Opin Biotechnol*, 40, 41-48.

STADLER, M., SCHERZER, M., WALTER, S., HOLZNER, S., PUDELKO, K., RIEDL, A., UNGER, C., KRAMER, N., WEIL, B., NEESEN, J., HENGSTSCHLÄGER, M. & DOLZNIG, H. 2018. Exclusion from spheroid formation identifies loss of essential cell-cell adhesion molecules in colon cancer cells. *Sci Rep*, 8, 1151.

SURESH, M. V., BALIJEPALLI, S., SOLANKI, S., AKTAY, S., CHOUDHARY, K., SHAH, Y. M. & RAGHAVENDRAN, K. 2023. Hypoxia-Inducible Factor 1α and Its Role in Lung Injury: Adaptive or Maladaptive. *Inflammation*, 46, 491-508.

SUTHERLAND, R. M. 1988. Cell and Environment Interactions in Tumor Microregions: The Multicell Spheroid Model. 240, 177-184.

TIDWELL, T. R. 2021. 3 D in vitro cancer models for drug screening.

TIE, X., WANG, J., WANG, Y., FU, B., WANG, C., LI, X., JIA, Q., WANG, F., CHEN, S. & ZHANG, Y. 2023. The prognostic effect of metastasis patterns on overall survival in organ metastatic lung adenocarcinoma. 102, e33297.

VAN ZIJL, F., KRUPITZA, G. & MIKULITS, W. 2011. Initial steps of metastasis: cell invasion and endothelial transmigration. *Mutat Res*, 728, 23-34.

VAUPEL, P. & MULTHOFF, G. 2021. Revisiting the Warburg effect: historical dogma versus current understanding. 599, 1745-1757.

VISHWAKARMA, M., DI RUSSO, J., PROBST, D., SCHWARZ, U. S., DAS, T. & SPATZ, J. P. 2018. Mechanical interactions among followers determine the emergence of leaders in migrating epithelial cell collectives. *Nat Commun*, 9, 3469.

WARENIUS, H. M. 2023. The essential molecular requirements for the transformation of normal cells into established cancer cells, with implications for a novel anti-cancer agent. *Cancer Rep* (Hoboken), 6, e1844.

WEBER, S. & BAUER, U.-M. 2009. Arginine methylation in interferon signaling: New light on an old story. *Cell Cycle*, 8, 1461-1465.

WEINBERG, D. H. A. R. A. 2000. The Hallmarks of Cancer. Cell.

WIIG, H. & SWARTZ, M. A. 2012. Interstitial Fluid and Lymph Formation and Transport: Physiological Regulation and Roles in Inflammation and Cancer. 92, 1005-1060.

WIIG, H., TENSTAD, O., IVERSEN, P. O., KALLURI, R. & BJERKVIG, R. 2010. Interstitial fluid: the overlooked component of the tumor microenvironment? Fibrogenesis & Tissue Repair, 3, 12.

WU, J. S., JIANG, J., CHEN, B. J., WANG, K., TANG, Y. L. & LIANG, X. H. 2021. Plasticity of cancer cell invasion: Patterns and mechanisms. Transl Oncol, 14, 100899.

XIAO, Y. & YU, D. 2021. Tumor microenvironment as a therapeutic target in cancer. *Pharmacology & Therapeutics*, 221, 107753.

YAMAZAKI, D., KURISU, S. & TAKENAWA, T. 2005. Regulation of cancer cell motility through actin reorganization. 96, 379-386.

YANG, D., LIU, J., QIAN, H. & ZHUANG, Q. 2023. Cancer-associated fibroblasts: from basic science to anticancer therapy. *Experimental & Molecular Medicine*, 55, 1322-1332.

YANG, G., WANG, H., FENG, M., YOU, L., ZHENG, L., ZHANG, T., CONG, L. & ZHAO, Y. 2019. Integrated analysis of gene expression and methylation profiles of novel pancreatic cancer cell lines with highly metastatic activity. *Science China Life Sciences*, 62, 791-806.

YANG, Y., ZHENG, H., ZHAN, Y. & FAN, S. 2019. An emerging tumor invasion mechanism about the collective cell migration. *Am J Transl Res*, 11, 5301-5312.

ZANONI, M., PICCININI, F., ARIENTI, C., ZAMAGNI, A., SANTI, S., POLICO, R., BEVILACQUA, A. & TESEI, A. 2016. 3D tumor spheroid models for in vitro therapeutic screening: a systematic approach to enhance the biological relevance of data obtained. *Scientific Reports*, 6, 19103.

ZHANG, J.-L., LIU, Y., YANG, H., ZHANG, H.-Q., TIAN, X.-X. & FANG, W.-G. 2017. ATP-P2Y2-β-catenin axis promotes cell invasion in breast cancer cells. 108, 1318-1327.

ZHAO, J., DU, F., LUO, Y., SHEN, G., ZHENG, F. & XU, B. 2015. The emerging role of hypoxia-inducible factor-2 involved in chemo/radioresistance in solid tumors. Cancer *Treatment Reviews*, 41, 623-633.

ZHAO, W., ZHAO, H., LI, M. & HUANG, C. 2020. Microfluidic devices for neutrophil chemotaxis studies. *Journal of Translational Medicine*, 18, 168.